ADDITIVE MANUFACTURING OF TECHNICAL CERAMICS

Master degree in Product Design Engineering

António Miguel Rocha Raimundo da Silva

Leiria, March of 2019

ADDITIVE MANUFACTURING OF TECHNICAL CERAMICS

Master degree in Product Design Engineering

António Miguel Rocha Raimundo da Silva

Dissertation under the supervision of Doctor Fátima Barreiros, professor at School of Technology and Management from Polytechnic Institute of Leiria, and co-supervision of Doctor Teresa Vieira, professor at Faculty of Sciences and Technology from University of Coimbra.

Leiria, March of 2019

Originality and Copyright

This dissertation report is original, made only for this purpose, and all authors whose studies and publications were used to complete it are duly acknowledged.

Acknowledgments

Considering that the realization of this work would not be possible individually, I would like to acknowledge:

Professor Fátima Barreiros, for suggesting such an actual and challenging theme. I would like to thank her for all the support and supervision, as well as the sharing of her deep scientific knowledge.

Professor Teresa Vieira, for all the guidance, all the shared knowledge and all the motivation given in the search of the best results possible.

CDRsp and IPN, for the willingness to open their laboratories and letting me to perform all the different tests.

Fábio Cerejo, for being a great laboratory partner and for the help given in the course of this work.

Palbit©, for giving me the material to work with and for being able to sinter the produced parts.

Lastly, but not least, my family and to Susana, for all the support and motivation to overcome all the challenges.

To all,

My sincere thanks!

Abstract

Additive Manufacturing (AM) is an area intrinsically linked to industry 4.0 because of its ability to meet some of the most significant challenges in the industry such as production of custom parts, complex geometries and direct processing (through cloud manufacturing). Due to its advantages, the market for functional parts based on inorganic materials via AM is in great development.

The present study has focused on the Fused Deposition of Ceramics (FDC) process, which is suitable, in combination with post-processing steps such as debinding and sintering, for the consolidation of ceramic powder particles from filamentary materials. Although the volume content of ceramic powders is very limited, due to the absence of high pressures, the FDC has been of scientific and industrial interest due to its ability to eliminate some limitations imposed by other processes such as Selective Laser Melting (SLM), due to the sources of high energy consumption, and Powder Injection Molding (PIM), due geometric and mold cost limitations.

The major challenges of this dissertation involved producing filaments for FDC, based on PIM or powder extrusion (PE) methodologies, joining the filaments of feedstock with optimized ratios of tungsten carbide powder (48.5%vol.) that should withstand the stresses involved in the FDC extrusion, and providing suitable extrusion fluidity. Afterwards, the challenges were overcome and the shaped parts through FDC were debinded and sintered. These processes led to the production of near net shape WC-10Co parts with characteristics and properties close to those resulting from conventional replicative processes of the powders.

Keywords: *FDC, Filament, Feedstock, Binder, Powder; WC-10Co*

Contents

List of Figures

List of Tables

List of Symbology & Acronyms

Symbology

BF1	Binder Formulation 1
BF2	Binder Formulation 2
WC-10Co	Tungsten Carbide with 10% Cobalt
WC-20Co	Tungsten Carbide with 20% Cobalt

Acronyms

ADM	Additive Digital Manufacturing
AM	Additive Manufacturing
BJ	Binder Jetting
CAD	Computer Assisted Design
CPCV	Critical Powder Concentration Volume
DPD	Direct Powder Deposition
EBM	Electron Beam Machining
FDM	Fused Deposition Modeling
FDC	Fused Deposition of Ceramics
FDMet	Fused Deposition of Metals
HIP	Hot Isostatic Pressing
IFM	Infinite Focus Microscope
IP	Inkjet Printing
LMD	Laser Metal Deposition

PIM	Powder Injection Molding
RP	Rapid Prototyping
SA	Stearic Acid
SEM	Scanning Electron Microscope
SLA	Stereolithography
SLM	Selective Laser Melting
SLS	Selective Laser Sintering
TGA	Thermogravimetric Analysis
TPE	Thermoplastic Elastomer
XRD	X-Ray Diffraction

1. Introduction

The present study aims to demonstrate the work developed in the scope of additive manufacturing process (AM), namely Fused Deposition of Ceramics (FDC), which is based on the well-known process called Fused Deposition Modeling (FDM), using technical ceramics. Throughout this work the study strove for the development of a ceramic feedstock suitable to that particular AM process (FDC).

This study will present various techniques used to develop, mix and characterize ceramic feedstocks suitable for the FDC process. Afterwards, it will discuss the production of parts on different geometries, with different complexities, including 3D printing and sintering steps.

In the present study, the material is tungsten carbide with cobalt as metal binder, mixed with a polymeric binder system, extruded into a filament shape. The production of the filament feedstock was optimized by torque rheometry, allowing the filament to be easily extruded. The 3D printing conformation of parts/systems were supported in a commercial grade FDM printer. Thermal debinding and sintering were made in industrial conditions that allow sound, easy and economical parts. After the sintering stage, tungsten carbide parts were obtained with success.

1.1. Engineering Context & Motivation

With the increasing pressure imposed on industries to achieve more optimized processes and products capable of responding to more solicitations, there has been an increase in developing more complex components using highly technical materials. Another aspect that has also been rising the interest of industry and academy is the development of new processes capable of overcome the needs of industry 4.0, namely the production of optimized components, both topologically and geometrically.

The present work focuses on the design, materials and processes for the manufacturing of technical ceramics with complex geometries. Through new production methods, namely AM, different materials must be studied in order to attain the objectives of the fourth industrial revolution, promoting the optimization and sustainability of the developed products.

Nowadays, with regard to the technological developments of design, simulation, and processing, a great effort is being done to develop materials suitable for additive manufacturing, in academic or industrial sections.

With respect to manufacturing technologies, the additive processes, in particular the fused deposition modeling technologies for 3D printing, exhibits a processing configurations that place them at the forefront as manufacturing methods, to produce parts with complex geometries.

Developing materials that are suitable for producing complex shape with functionalities is pre-requisite for AM techniques. These developments provide manufacturing facilities for industries, moreover, techniques that require less energy consumption and decreases wastes from processing stages, without compromising shape and function, are in line with the objectives recognized for the fourth industrial revolution. Being able to produce parts through FDC, using materials like tungsten carbide, allows companies, namely the cutting tools industry, to develop new and customized solutions for their requirements for a competitive price.

1.2. Objectives

The present work has a main objective that includes the development and study of the fundamentals for the design and production of filaments composed of technical ceramic, WC-Co, for an additive manufacturing process. The use of filament materials for additive extrusion processes allows the creation of structures with complex geometries, which can not be replicated by conventional processes without the need of high consumption energy and additional costs.

For the implementation of the additive manufacturing process, the use of an additive extrusion process is intended, using a filament based on a feedstock of inorganic ceramic powders with a binder system (polymers, organic acids…), in order to produce parts by a controlled deposition technique.

The objectives of this work can be divided into different steps. The first one is mainly developping a ceramic filament material suitable for additive manufacturing. With regard to this objective, the following specific objectives are emerged:

- Development and characterization of powder-binder feedstocks suitable for the production of the filament to be processed by FDC;
- Production and characterization of FDC parts (green parts);
- Application of thermal treatments on the green parts and their characterizations;
- Evaluation and discussion of results.

Thus, different experimental techniques will be applied to produce and characterize filaments and parts in different stages of production. Moreover, it will be possible to demonstrate that FDC is suitable to tailor products of WC-Co, with properties similar to those resulting from conventional methods, allowing a future production of complex geometries with WC that otherwise were not possible.

1.3.Dissertation Structure

This dissertation is divided into 5 chapters:

1. Introduction;
2. State of the art;
3. Materials and experimental procedures;
4. Experimental results;
5. Conclusions and future works.

In the first chapter, a brief introduction to the theme is described, as well as the motivation for the accomplishment of this work and the proposed objectives for its development.

The second chapter is dedicated to the state of the art, where a bibliographic review related to the proposed theme is done with greater emphasis on the additive processes of ceramic materials. In this chapter, an approach to the innovative features of this work is made.

In the third chapter, the case study of this work is presented, which describes the materials characterization and the experimental procedures performed, reporting all the stages related to the development of the experimental work.

The fourth chapter is reserved for the presentation and discussion of the results obtained in the experimental work, in order to validate the different hypotheses addressed throughout the study.

Finally, the fifth chapter points out the general conclusions of the study and suggestions for future works related to the studied subject.

2. State of the art

Taking into account the objective of the present work, the state of the art reflects the main topics related to the development of a suitable filament of ceramic material for FDC and their behaviour during the process. Therefore, an overview of the evolution of additive manufacturing techniques will be firstly presented, with its respective framing, followed by an approach to the FDM process, which will serve as the basic technique for the production of the ceramic component. After presenting the FDM process, the specific technique to produce ceramic parts, the FDC, will be addressed, concluding with the materials analyses to obtain a final product.

2.1. Additive Manufacturing: History and Overview

Additive Manufacturing (AM) comes as a set of techniques capable of responding to constraints in conventional processing techniques. AM involves the binding of material to produce components through the application of computer assisted design 3D (CAD) models, usually layer-by-layer, allowing the efficiently construction of small or big components with complex geometries. Unlike conventional manufacturing, the cost of producing products using AM is not affected by product complexity or lot size, as shown in Figure 1 [1].

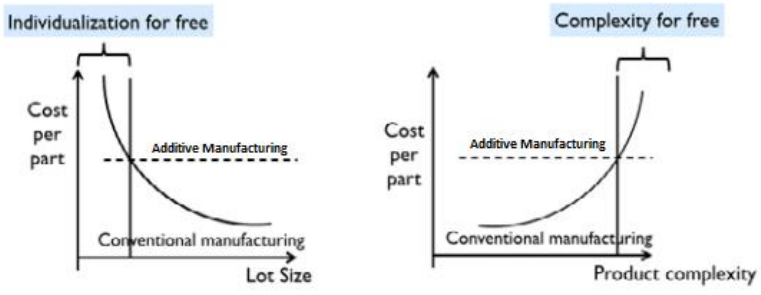

Figure 1 - Conventional manufacturing vs. Additive manufacturing [1]

Thanks to the digital nature of the processes involved - CAD development, and communication between the equipment and the various CAD software, the AM allows communication through the cloud (Cloud Manufacturing / Cloud Production). The equipment can print a CAD file that is in any other location, minimizing the costs of transportation and storage of the various materials involved in its production [2]. The simplicity of file and step management offered by AM is an asset in an industrial context. Moreover, in the context of the objectives of the 4th revolution (Industry 4.0), it adds value in the access to finished parts by the domestic user, a market segment that has been evolving through the development of the technologies inherent to this manufacturing process. In Figure 2 it is possible to observe a set of steps, common to several business models, which are reduced through AM [3], [4].

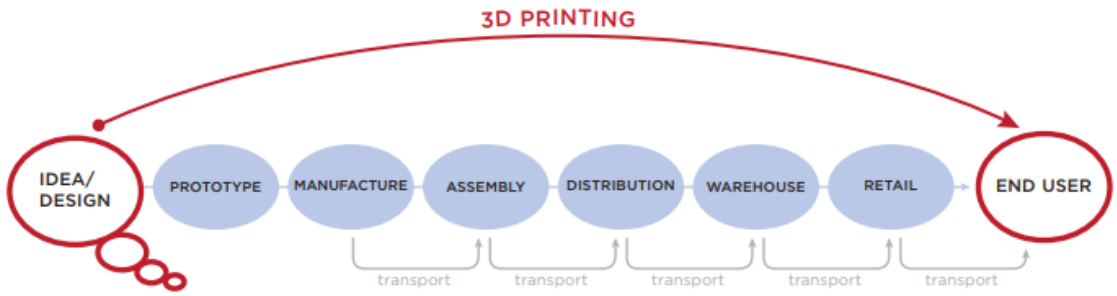

Figure 2 - Steps in conventional processes vs. additive processes (adapted from [3])

With constant technological developments, through the diversification of applications and the reduced environmental impact, the future of AM is promising, since it has been increasingly adopted by large companies to solve old problems. Figure 3 shows some of the present and future applications of additive manufacturing technologies.

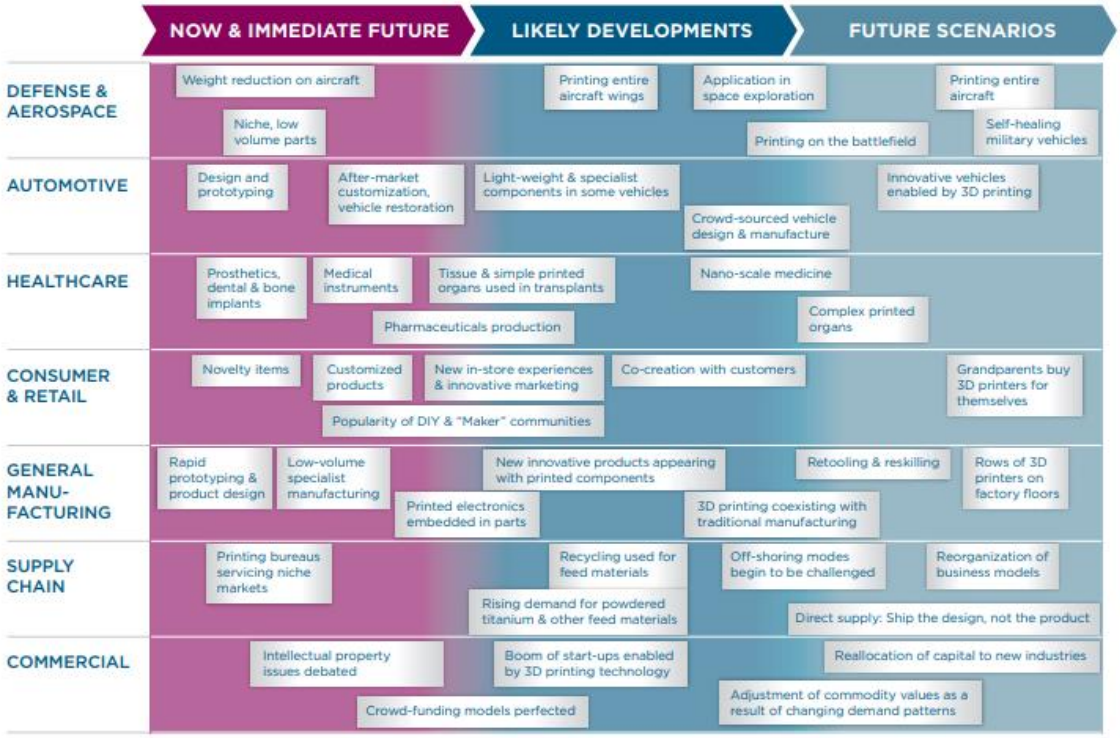

Figure 3 - Current and future applications for additive manufacturing technologies (adapted from [3])

In order to be able to produce complex geometries, Hideo Kodama of the Municipal Institute of Industrial Research of Nagoya [5], in 1981, developed a rapid prototyping system that used a UV light projector to harden a photopolymer, constructing a part through the sequence of various exposures, layer-by-layer. Based on this work, in 1984, Charles Hull developed the first patented additive three-dimensional construction process, stereolithography (SLA) [6], [7]. This being the case, additive manufacturing quickly became the subject of studies in order to diversify the type of processes and the type of used materials. Therefore, due to the ease of processing, polymers were preferred to be used initially, giving rise to the evolution of different AM processes. Preliminary machineries were based on SLA system, using photopolymers and UV projectors, however, based on different techniques to process polymeric materials, new technologies were quickly introduced on the market [7]. Initially, the photopolymers were presented in liquid state in order to be cured via UV, however, new materials for AM purposes began to appear in the form of granules, filaments and even

powders [5], [7]. Based on these new materials, new processes were developed such as Fused Deposition Modeling (FDM), in 1991, by Stratasys [7], which uses filament material; Selective Laser Sintering (SLS), in 1992, by DTM, later acquired by 3D Systems, which uses material in the form of powder; and Inkjet Printing (IP), in 2000, by Object Geometries and Z-Corp [7], which also uses material in the form of powder and liquid binder.

Due to changing attitudes towards the development of low cost additive production systems, a growth in the dissemination of additive technology for the business sections formed, as shown in Figure 4 [8].

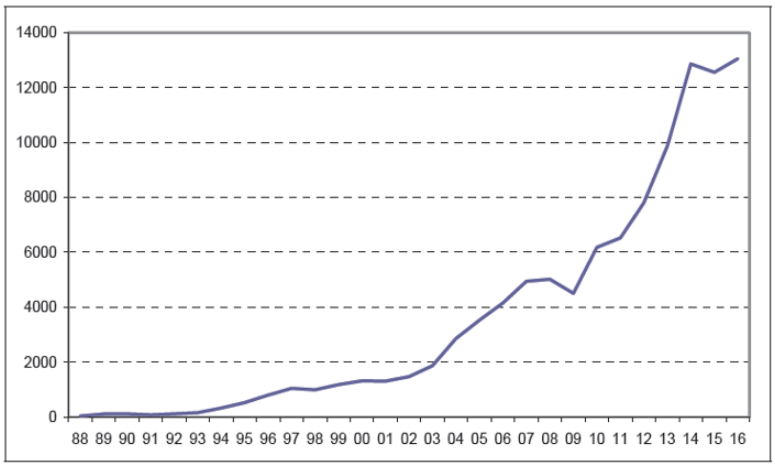

Figure 4 - Number of AM equipment in industry vs. year (adapted from [8])

The increase in the use of AM processes led to a cycle of development and brand creation, based on different technologies, which allowed the additive manufacturing market to expand even further along the industry, creating opportunities for the processes to be evolved accordingly to the needs of industries [8].

With the maturation of additive processing technologies using polymers, concepts such as "Rapid Prototyping" (RP) were introduced, which designated the set of operations and the parts obtained through additive manufacturing. The products were considered rapid prototypes, since the functional or structural characteristics did not have the desired properties [9]. An example of this is the production of prototype parts for design verification

purposes in a physical model, or the production of mechanical systems, using polymers instead of metals, to carry out proofs of concept.

Through the development of new techniques suitable for the AM of polymers, the scientific community has focused its attention on the development of additive techniques allowing the processing of metallic and ceramic materials, due to the great interest of the industry. Conventional shaping processes used in industrial environment, such as Powder Injection Molding (PIM), a derivation of injection molding, already had available ceramic and metallic materials [10], [11], but geometric/size constrains and mold cost did not allow enough flexibility for the process.

The focus of the industry on the use of metallic and ceramic materials, oblige to the development of processes that allow building freeform parts. Thus, it must be highlighted Laser Melting (SLM), where a powder bed and a laser that melts powder, developed by F&S Stereolithographietechnik GmbH (later SLM Solution GmbH); Electron Beam Melting (EBM) where an electron beam is the heat source, developed by Steigerwald Strahltechnik GmbH; and Direct Powder Deposition (DPD), developed by Gnanamuthu, denominated by laser cladding [1], [12]. These processes approached additive manufacturing with a new perspective, using high-power energy sources to melt small metal particles, layer-by-layer, in order to produce high-densification metal components. In the field of additive metal production, SLM has been the most used to produce metal parts due to the possibility of processing various metallic materials and obtain parts with mechanical properties similar to those obtained with conventional processes. However, this process presents high-energy consumption, due to the use of lasers, added risks to the technician who operates the equipment, and the presence micropowders (<50µm). Also the manufacturing cost is high, due to the material cost, and surface finish that may not be in according to the requirements of some industries (i.e. mold making industry) [13].

Although the processes mentioned before have become the basis of the metallic additive processes, new methods of producing metals and ceramics have being studied, like Fused Deposition of Metals (FDMet) or ceramics (FDC), in the case of processes that derive from FDM, or even processes like Laser Metal Deposition (LMD), which derives from DPD.

FDMet and FDC are growing processes, which are increasingly accessible to common users and companies, because they offer the opportunity to create parts easily at a low cost. Thus, it becomes important to study these techniques.

2.2.Fused Deposition Modeling

FDM is one of the world's most widely distributed additive manufacturing technique because of its reliability, operation safety, simplicity, large quantity of available material diversity and low material waste [13]. In this type of technic, a continuous filament of material produced by an extrusion head, heats the material to its softening temperature. The material is extruded onto a platform or onto the previously deposited layer, having this process repeated layer-by-layer until the final part is completed (Figure 5) [9], [13]–[21]. The extrusion head can be divided into two zones, one hot and the other cold. It is through the cold zone, corresponding to the upper half of the extrusion head, where the filament enters. In this zone, there is a stepper motor, pulling the filament of material from the feed zone to the extrusion nozzle. This motor rotates in small precise rotations, as intended, to deposit the material in the exact amount. The drive gear has the function of pulling the filament so that it moves in accordance with the rotational movement of the engine. Gear reducer obliges to the load applied to the filament increases, enabling its transport. This mechanism may be or not in the extrusion head. If not, it is an isolated component. The filament guide is a single tube that guides the filament of material directly to the extrusion nozzle. The separation between the hot and cold zones is made by a thermal insulator, which must be designed in order to allow the passage of the filament from one zone to another but avoiding heat flow from one side to the other. It is in the hot zone that the filament is softened and extruded, by the extrusion nozzle subsequently. There is an electric resistance in this zone, which surrounds the filament on its passage, enabling the adequate viscosity of the filament during its deposition. In addition, in the extrusion nozzle there are also temperature sensors to control the temperature of the filament, in order to confirm that the temperature is correct for the material, and allows its regulation if this does not occur. The temperature of the head and the extrusion nozzle is an important factor in ensuring that the material, remains

at the same temperature when extruded, avoiding different cooling rates, preventing bending and maintaining a uniform layer. The extrusion head moves along the X-Y plane and by CAD the deposition layer by layer of material, is carried out. When a complete layer is produced, the platform moves along the Z axis according to the layer thickness, and starts the extrusion of a new layer [8], [18], [22]–[24].

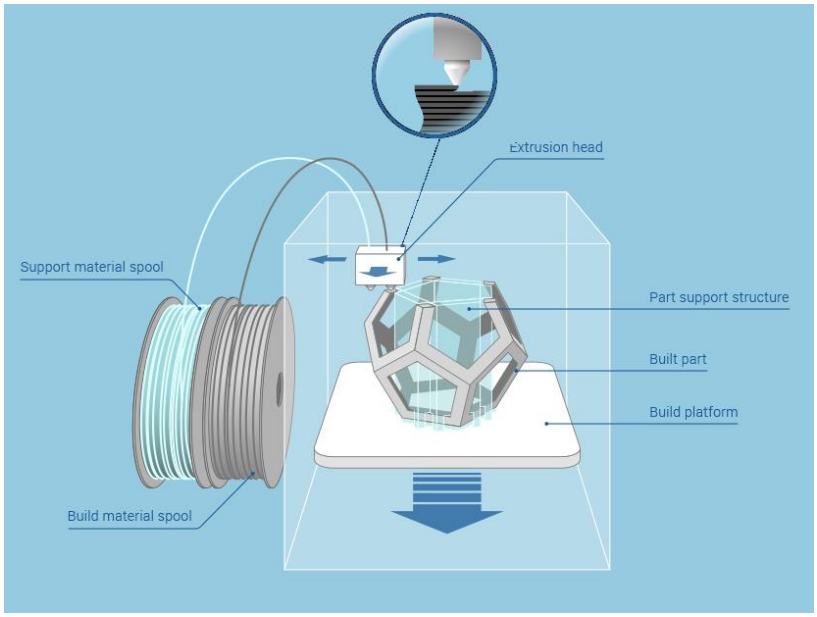

Figure 5 - Scheme of the FDM process (adapted from [25])

Due to its simplicity, safety, reliability and low energy consumption, the FDM process has been widely distributed for domestic use. This equipment represents the majority of the market share, as well as being the subject of constant improvements and adaptations to meet the needs of the various industries [26]. Figure 6 shows the domestic market shares, as well as the business ones, related to additive production techniques. According this figure, it is evident the predominance of FDM techniques.

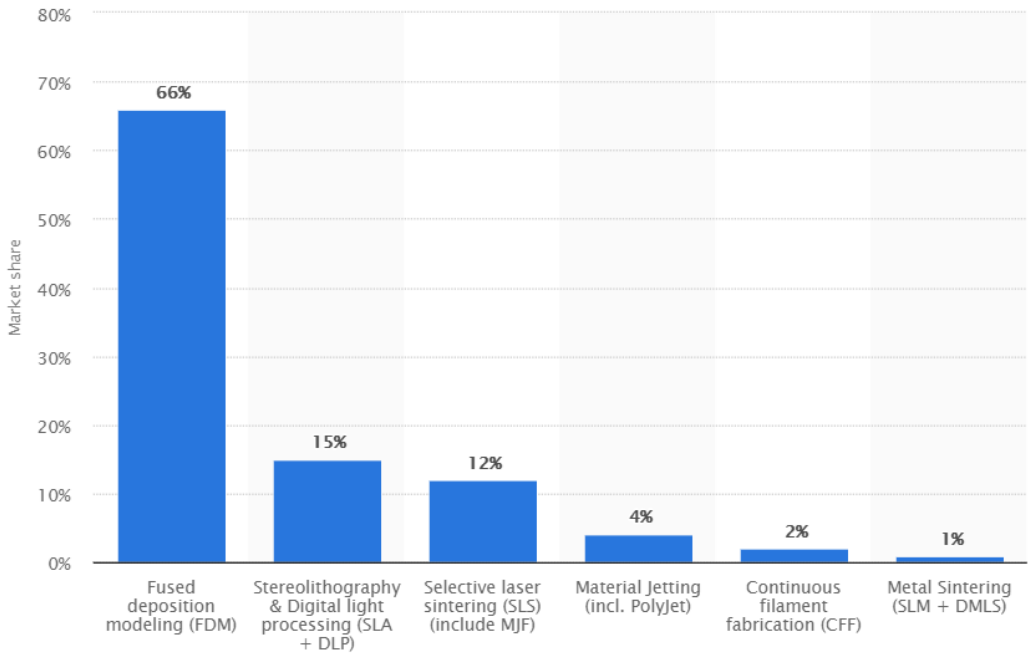

Figure 6 - Market Share for 3D printing technologies worldwide [26]

According to its global presence, the FDM process has been the subject of several studies, in order to optimize and increase the range of materials produced, namely metals and ceramics, leading to processes such as FDMet or FDC [7], [27]. The study of this type of techniques led to, as main objective, the development of complex functional parts, made them increasingly move away from the concept of "Rapid Prototyping" (RP) to what is now called as "Additive Digital Manufacturing" (ADM) or "AM" [28].

2.3.Fused Deposition of Ceramics & Metals

The FDC process is derived from the FDM technique, as described in the U.S. Patent 5738817 [29], using a feedstock (homogeneous mixture of a ceramic material with a polymeric binder) that must present adequate fluidity during the extrusion process [27], [29]–[32]. After extruding the desired part, composed by the feedstock (green part), it is necessary to carry out binder removal (brown part) and sintering (final part), assuring the required geometrical and mechanical properties [20], [33]. The extrusion step is analogous to that of the FDM process.

The FDC additive extrusion has been developed to suppress some of the limitations of processes using ceramic materials, like PIM or Binder Jetting (BJ) [19]. Figure 7 presents some of the limitations related to the PIM and BJ processes, which are intended to overcome with the FDC technique.

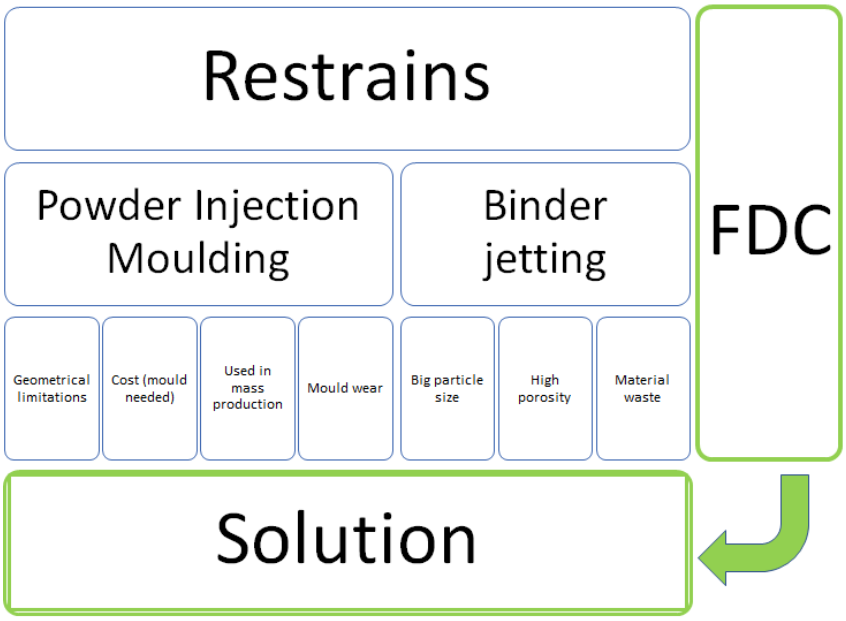

Figure 7 - PIM & Binder jetting disadvantages (adapted from [19])

In order to use FDC in the production of parts, there are several steps that must be followed. In Figure 8 it is possible to observe the steps related to the development and processing of parts via FDC.

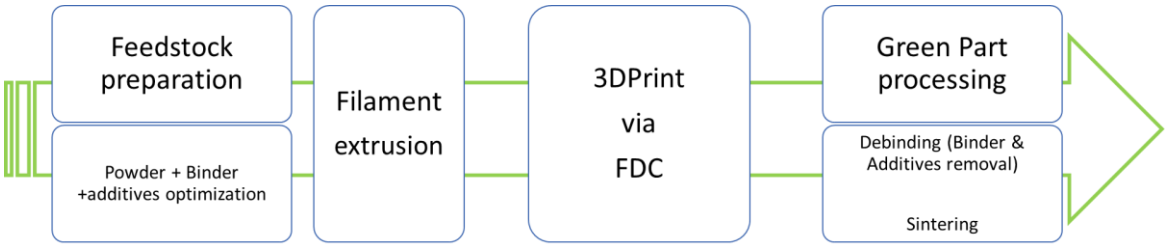

Figure 8 - FDC process flowchart (adapted from [30])

In the FDC process, the preparation of the filaments is a crucial step, because this must present high strength and low viscosity to allow extrusion. On the one hand, as FDC uses small step motors to extrude, the pulling force is small, meaning that the filament strength plays a fundamental role, allowing it to act like a piston during extrusion and preventing it from bending or breaking. On the other hand, as the filament extrusion must flow at a constant rate, it must present low viscosity, with adequate flowability, to avoid the return of the heated filament to the inlet of the extrusion head [20], [24], [31]–[34].

The production of parts using FDC has been growing, with more and more developed materials suitable for this technique. In general, the FDC process uses filament, however, there are studies that use a different approach in the construction of the extrusion head, which makes possible to extrude granular material using a screw. This technique allows to extend the range of materials, since the mechanical stresses involved in the extrusion are higher [35].

In the same way as FDC can use different extrusion head mechanisms, FDMet also adopted different solutions for the extrusion process, with company's developing new machine systems, such as DesktopMetal® or Markforged®. The equipment's developed by these company's uses a rod-shaped material that is fed through cartridges, using a small cylinder and vertical movement, to create pressure in the rod, making it to pass through the extrusion head. In this way, this equipment allow an increased amount of powder in the feedstock, because the viscosity does not need to be as low as that required for a filament, thus allowing to decrease the complexity of the formulation of the feedstock [36]. Figure 9 displays three different types of extrusion heads used in FDC and FDMet processes.

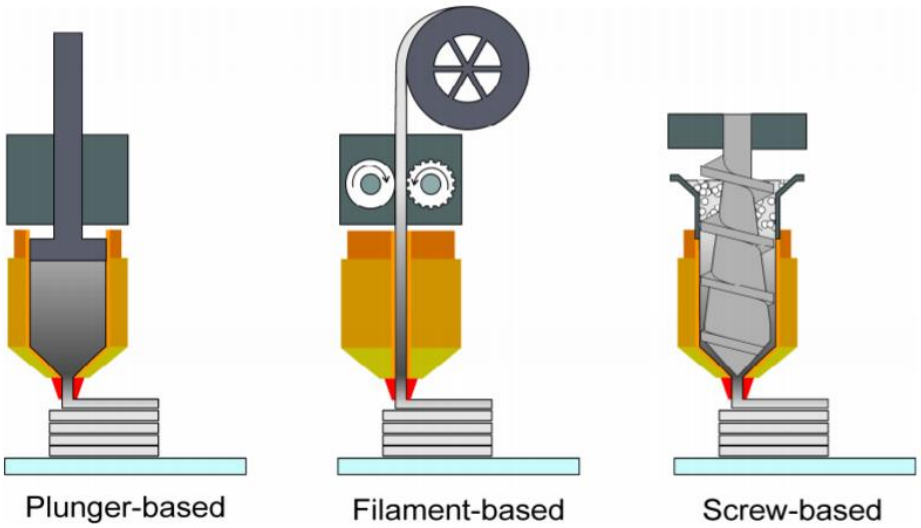

Figure 9 - Additive Extruder types (adapted from [34])

Despite the developments made to equipment–and feedstock pre-processing, the use of filaments to feed the extrusion process is still preferred, and, until now, studies have been carried out with the objective of producing filaments with materials such as silicon nitride, silica, piezoelectric ceramics, alumina and tungsten carbide [20], [33].

Thus, it is essential to understand what properties must be studied and controlled, to attain a homogeneous mixture suitable for additive extrusion parameters and the required properties for the final part. Regarding this, the following sections describe the most important parameters of the raw materials used for the formulation of the feedstocks, namely powder and binder, the properties that the feedstocks must present and, finally, some concerns related to the final treatments of debinding and sintering.

2.3.1. Ceramic Powders

The ceramic powder is a critical material for the feedstock, since its properties have a direct influence on both mixing and process behavior. Regarding the selection of the ceramic powder, it is necessary to consider fundamental parameters, sometimes referred in the literature as "Powder 5S" (Shape; Size; Particle Size Distribution, Structure and Surface) [37]. A powder whose shape comes from a fine granulation process and whose particle size

distribution is wide allows to lower the viscosity of the feedstock [20]. Powders influence the microstructure of the green product and the decomposition of the binder and affect the presence of defects during its elimination. Its structure and shape influence the packing rate, which has a direct relation with the binder elimination, because the spaces that are not occupied by powders will be occupied by the binder. Thus, it is necessary that the powders have a wide and well-defined distribution and a morphology as close as possible to the sphericity, because it will allow a greater contact area between the powder and the binder and higher packing rates [38]–[40]. Powder shapes different from spherical, particularly laminar shapes, besides not promoting a good adhesion between the binder and the powder, can induce internal stresses [37], aligned with the direction of the powder surface, which after sintering can originate cracks in the part.

2.3.2. Binder

The binder system, in general, includes one or more organic constituents to form a mixture, which may be based on thermoplastic or thermosetting polymers and other additives, namely waxes, which can be partially soluble in water or organic solvents. Generally, for producing feedstocks for FDC, thermoplastic binder systems are preferred. The binder formulation depends on a number of factors, including the materials compatibility, the viscosity required for the filament deposition, the compressive strength (affected by the feed systems and the material in the extrusion nozzle) and the flexibility necessary to create a filament [20], [29].

Thus, the binder is constituted by several components, usually a polymer that will function as the backbone of the system, not only ensuring that the ceramic particles remain together in the sintering step, but also guaranteeing some resistance and stiffness; the waxes that will be used to lower the overall viscosity of the binder; the plasticizers used for promoting flexibility/hardness of the binder; and the adhesion enhancing constituents. The various organic components, which constitutes the binder, are divided into 3 groups: 1) master binder; 2) backbone polymer; 3) additives [29].

Besides the influence of the binder on the processing of the material during extrusion, it also influences one of the most critical stage of the process, the debinding stage. The properties

of the final parts obtained after sintering will also be greatly influenced by the former stages, and the final part will be a “mirror” of their suitability [41].

2.3.3. Powder/Binder Mixtures

It is always desirable when the filament is developed that the solids content is as high as possible without compromising the rheology of the mixture to avoid defects in the extrusion and processing of the "green" body [20], [33], [37]. As with PIM materials, the preparation of the powder/binder feedstock begins with the optimization of the volumetric fraction of solids (Critical Powder Volume Concentration - CPVC), which is defined by the ratio of the volume of powder to the total volume of binder and powder [37]. The admissible percentage of solids in a feedstock is related to the greater or less ease of packaging of the particles, since the space between them should be filled by binder. In this way, it becomes fundamental to know the critical volume concentration of powder, selecting a suitable concentration such that the viscosity of the feedstock enables its flow and allows the interaction between particles in order to ensure the preservation of the shape of the part during processing [11], [42]. According to the literature [21], [43], [44], the quantity of the inorganic material, in this case ceramic powder, in the feedstock, is about 45% to 70% volume, however, in several literature [20], [33], [36], [42], [45], [46], the minimum amount recommended is 50%, being the average range of powder content should be from 50 to 65% (%vol). The amount of the inorganic material will have an impact not only on the final part, due to the sintering process, but also on the green part. The homogeneous distribution of the powder is fundamental to avoid the collapse of the part after the removal of the binder, before the sintering stage. In fact, a poor distribution can lead to the collapse of the structure in the debinding stage, or to the formation of porosities, for the least..

Figure 10 shows a typical example of the powder dispersion in a feedstock. It is possible to conclude that there is a homogeneous dispersion between powder and binder, and that the particle size distribution of the powder is wide, since different sizes of powders are present. The wide particle size distribution promotes a lower viscosity of the feedstock, which is essential for obtaining an extrudable filament through additive processes [37].

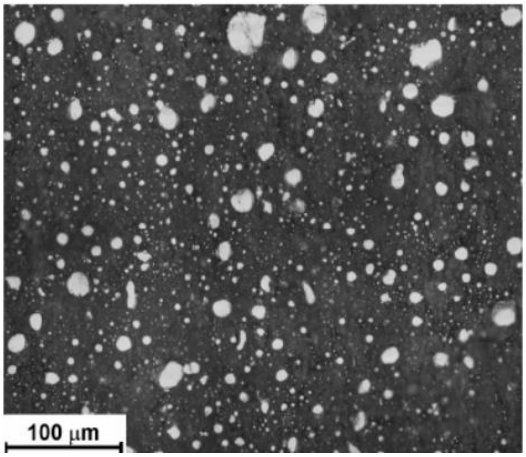

Figure 10 - Micrograph of feedstock showing powder surrounded by polymeric binder (adapted from [40])

According to the studies carried out by Kukla [46], the filaments should have a viscosity of about 1000 Pa.s, a modulus of elasticity of approximately 800 MPa to withstand approximately 40% of elongation before fracturing, as shown in Figure 11.

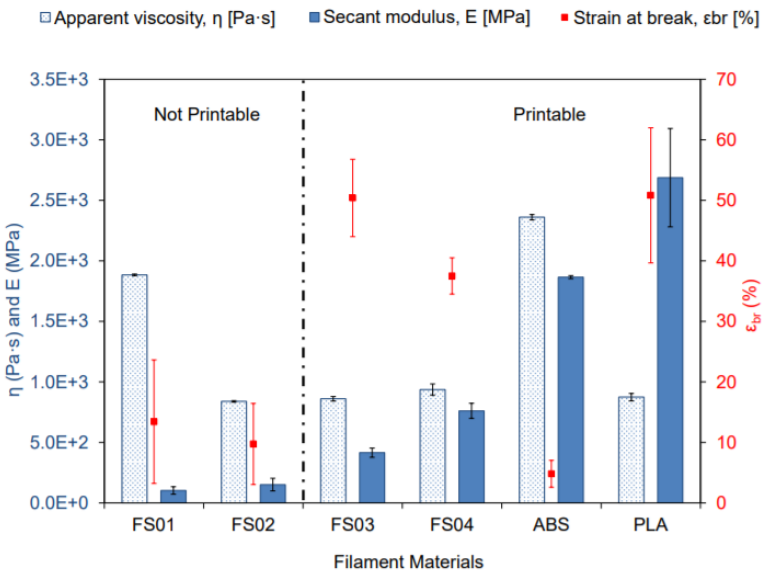

Figure 11 - Filament properties for additive extrusion (adapted from [46])

2.3.4. Debinding & Sintering

As previously described, the final part is obtained after the steps of debinding, in which a "brown" part will be obtained, and sintering. Figure 12 shows the feedstock transformation processes.

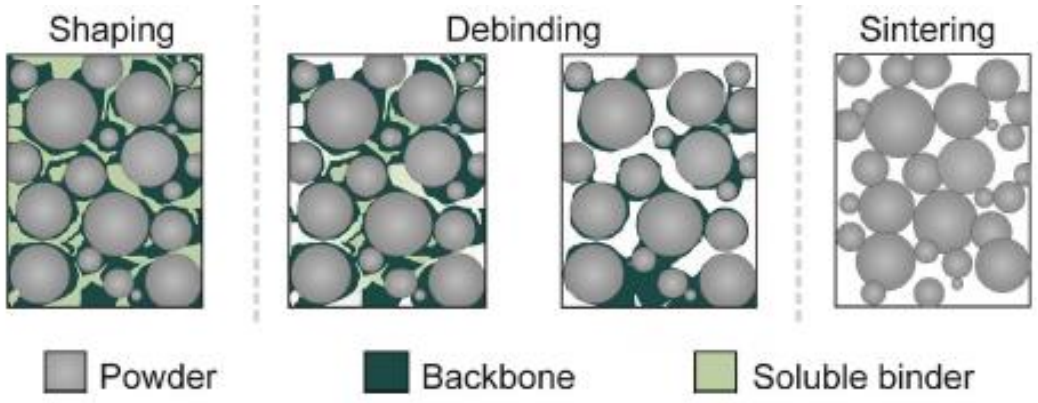

Figure 12 - Feedstock transformation process (adapted from [36])

The binder removal can be carried out using different approaches, as follows: solvent extraction, thermal decomposition, supercritical and catalytic debinding. This approach depends on the basic characteristics of the binders. However, thermal decomposition is the most common technique. In general, inert atmospheres are used for debinding, in order to avoid chemical reactions with the constituents used [43]. Regardless of the used process, the objective of debinding is to perform a quick and efficient removal of the binder, without inducing internal and/or external defects to the part, and ensuring that it maintains its three-dimensional shape [37]. Since several constituents, compose the binder, which causes different elimination kinetics; a partial and gradual degradation of the binder is needed.

In order to obtain a bulk part it is necessary to sinter the brown, materializing its densification. This step is done using a controlled atmosphere and sintering temperature approximately equal to the 2/3 of the melting temperature of the powder material [47]. After sintering, being carried out under optimum conditions, the final density is very close to the density of the bulk material. At this stage, due to the high porosity of the brown part, there

is a significant shrinkage of the part [48], [49]. Figure 13 shows a typical cycle curve for sintering a ceramic material (WC-20Co + 2% paraffin wax).

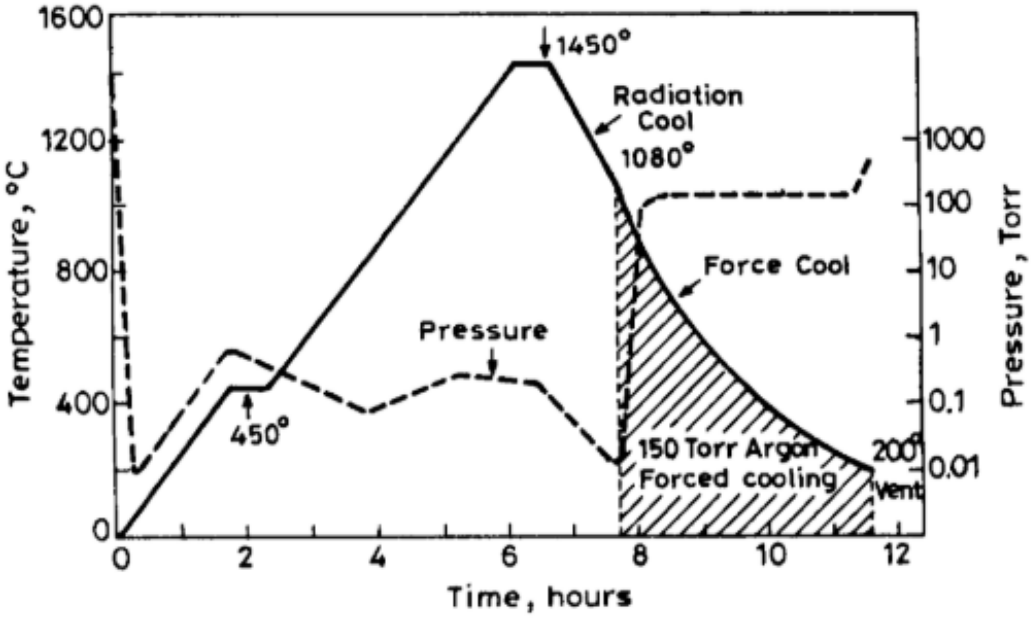

Figure 13 - Typical cycle curve for sintering WC-20Co + 2% paraffin wax (adapted from [47])

In order to carry out a correct sintering, the following aspects must be considered: sintering atmosphere, sintering temperature and holding time, heating and cooling rate. A well-defined process will lead to good results, minimizing the possibility of defects.

3. Materials and Experimental Procedures

In the present chapter the materials used in the aim of the experimental work will be presented, as well as the different procedures and techniques used to develop and characterize the feedstock, the produced filament and the final parts.

3.1. Raw Materials & Processing

Raw materials characterization provides vital information for material development, as it is fundamental to understand the material characteristics in order to attain a positive outcome. Powder and binder constituents will be characterized regarding the development of the filament. Feedstock preparation, filament extrusion and green part processing equipment's and parameters will be also presented.

3.1.1. Powder

Powder used in this work, was provided by a company dedicated to the manufacture of cutting tools. Thus, there was already data regarding some physical properties of the material. The powder provided was tungsten carbide with ten percent cobalt (WC-10Co). According the company information, the powder had a density of 14880 kg/m³, particles with an irregular shape, but with a shape factor close to 1, resulted from mechanical milling.

Additional tests were performed to characterize the powder. The median (d_{50}) and the cumulative particle size distribution (Figure 14) was evaluated using a laser diffraction particle size analyzer, the Mastersizer 3000 from Malvern Panalytical. This process measures the intensity of light scattered when a laser beam passes through a dispersed particulate sample, analysing this data in order to calculate the size of the particles that created the scattering pattern [50]. Since the powder is a mixture of tungsten carbide and cobalt, an X-ray diffraction (XRD) test was performed (Figure 15). XRD is a rapid analytical technique primarily used for phase identification of a crystalline material and can provide information on unit cell dimensions [51]. The equipment used was a Philips X'PERT from PANalytical with goniometer PW 3020/00, with a current intensity of 35 mA and an

acceleration tension of 40 kV. The anode was cobalt, with wave lengths $K\alpha_1$ = 0.17810 nm and $K\alpha_2$ = 0.17928 nm. The acquisition conditions were a step of 0.04º/s and acquisition time of 1 second, using a Bragg-Brentano (θ - 2θ) mount. Table 1summarizes the characteristics of the powder used.

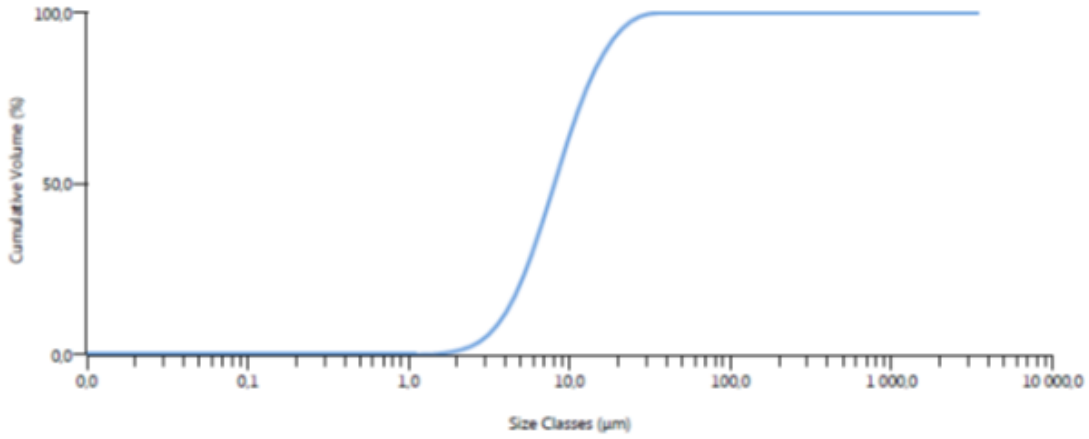

Figure 14 - Particle size distribution of WC-10Co

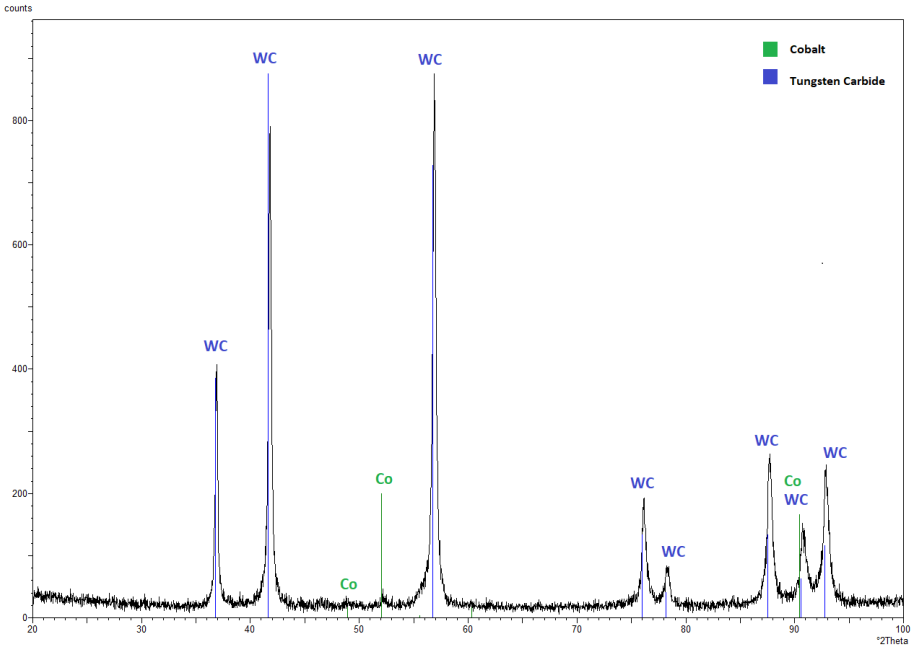

Figure 15 - X-ray diffractogram of WC-10Co

Table 1 - Powder characteristics

Powder	d_{10} (µm)	d_{50} (µm)	d_{90} (µm)	Density (kg/m^3)
WC-10Co	3.72	8.06	17.3	14880

After producing the filament, while studying the constituent's thermal behaviour, it was noticed that an excessive amount of polymeric mass was lost (3% more than expected). Thus, the thermogravimetric analysis (TGA) of the powder was performed to evaluate if any paraffinic wax was present, since it is a common practice to mix this waxes with tungsten carbide powders [47]. TGA was performed using the equipment TGA Q500 V20.13. Thermogravimetric analysis is an analytical technique used to determine a material's thermal stability and its fraction of volatile components by monitoring the weight change that occurs as a sample is heated at a constant rate [52]. The change in mass allows to evaluate the degradation temperatures of each constituent and the weight loss of each one. The heating rate used was 10°C/min under nitrogen atmosphere, to a maximum temperature of 800ºC (Figure 16).

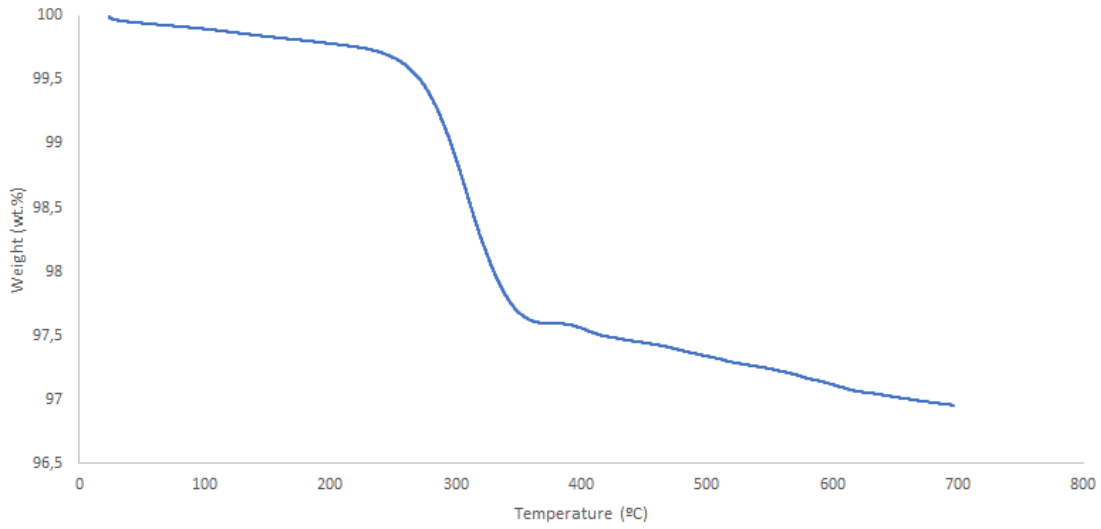

Figure 16 - TGA of WC-10Co

As it is possible to observe in Figure 16, the TGA revealed that 3% of the powder content degraded with temperature, revealing that it was a waxed powder. This result implied that the value of powder concentration considered when the evaluation of the critical powder volume concentration (section 4.1) was not the real one, since this wax content had not been accounted for in the previous calculations.

3.1.2. Binder

Since the binder is used in the feedstock as a temporary organic carrier of the powder, it is important to know the respective composition, since during its elimination, thermal cycles must be defined according the behavior of each constituent of the binder. As referred before, the various organic components of the binder are divided into 3 groups: 1) master binder; 2) backbone polymer; 3) additives.

In the present work, the master binder was a commercial grade binder, composed of a multipolymer blend of polyolefin and polyoxymethylene waxes (POM). Its use is based on several studies dedicated to PIM [42], due to its versatile nature, with different ranges of elimination temperatures according to the different constituents. The backbone polymer was a thermoplastic elastomer (TPE), linear triblock copolymer. The backbone polymer was used to improve flexibility of the feedstock in order to obtain a filament with adequate strength. Regarding additives, the surfactant used was stearic acid and the external plasticizer. The use of additives was mainly due to the high viscosity and low flexibility of the feedstock. Although stearic acid (SA) has been a common surfactant agent in PIM feedstocks, since it reduces inter-particle forces and lubricate the powder, improving its dispersion, the results in this experimental work showed that SA did not produce significant improvements on the feedstock developed, so it was decided not to use it in the final feedstock. Two different binder formulations were used in this study, as shown in Table 2.

Table 2 - Binder system characteristics

Formulation	Binder	Backbone	Additives	
			Plasticizer	Surfactant
Binder formulation 1 (BF1)	X %	X/5 %	Y %	Y %
Binder formulation 2 (BF2)	X %	X/5 % + 1/2Y %	Y % + 1/2Y %	N/A
Density (kg/m^3)	970	1030	970	980

As a controlled debinding process is fundamental to obtain high quality parts, it becomes critical to study the thermal behavior of both the binder constituents and the binder. In order to understand the degradation points of the various constituents, it was performed a thermogravimetric analysis using the TGA Q500 V20.13. The heating rate was 10ºC/min up to 500ºC. Figure 17 shows the degradation curves of the binder and of the M1 and TPE constituents. Using the TA Universal Analysis software, it was possible to obtain the onset and endset points of each constituent, as shown Table 3.

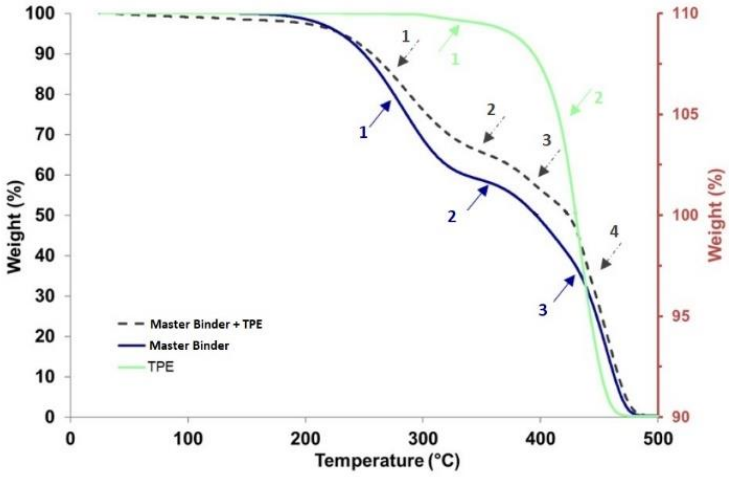

Figure 17 - TGA of the binder and of the master binder and TPE constituents

The TG curve of the master binder show three slopes (blue arrows), which correspond to the different constituents that constitute, such as POM and waxes. Therefore, those slopes evidence three degradation kinetics. At the final temperature, the residue is close to 0 wt.%.

TPE degradation curve show two distinct slopes (green arrows). The first slope corresponds to the evaporation of volatile softeners. At the final temperature, the ash content residue is also close to 0 wt.%.

The binder (POM&waxes+TPE) TG curve presents 4 significant degradation temperatures, where three of them are mainly attributed to the master binder (black arrows number 1, 2 and 4). The other degradation temperature (black arrow 3) is mainly due to TPE degradation and some of master binder residues.

Table 3 - Degradation temperatures and weight reduction of master binder, TPE and master binder+TPE

Binder TGA				
Binder constituents	Degradation Stage	Weight loss (%)	Onset (ºC)	Endset (ºC)
MasterBinder	1	52	232	314
	2	13	378	437
	3	46	437	472
TPE	1	2	300	327
	2	98	408	454
Master Binder+TPE	1	35	238	320
	2	11	375	398
	3	23	427	441
	4	31	450	475

3.1.3. Filament extrusion and green part manufacturing

The optimized feedstock was extruded into filament using a single screw extruder (Brabender GmbH & Co) with five controlled heat zones. The screw rotation was set at 5 rpm, with a 1.75 mm diameter nozzle, and the nozzle temperature was set on a range from 170 - 180ºC.

The green prototypes were produced in an opensource BQ Prusa I3 Hephestos 3D printer. The nozzle temperature was on a range from 200 - 215ºC. Extrusion multiplier has been set above 1 to compensate for the filament low diameter control, using as reference the standard 1.75 mm. Perimeter and infill strategies were adjusted to the filament 3D extrusion diameter to ensure that defects resulting from the FDC process would not have impact on the debinding and sintering phases. All the parameters were configured in Slic3r and all the files were generated using the Ultimaker Cura software.

3.1.4. Debinding & Sintering

The company that provided the powder (WC-10Co), Palbit®, performed the debinding and sintering of the green parts produced in the present work, using an industrial Hot Isostatic Pressing (HIP) oven. The thermal cycles used in the sintering process were the ones normally used by the company to sinter tungsten carbide for the cutting tool industry. In fact, using the same conditions of the company, the evaluation of the performance of both the filament production and the printing process was possible, since the thermal treatments are already optimised by the company. Two thermal cycles were used, namely: 1) heating up to 680ºC at hydrogen atmosphere to remove all the waxes, followed by heating up to 1485ºC at 25 bar pressure; 2) heating up to 1450ºC under 30 bar pressure.

3.2.Experimental Techniques for Characterization

In the present topic the experimental methodologies used in the optimization of the feedstock and in the preparation and processing of the filament are discussed.

3.2.1. Torque Rheometry

The feedstocks were optimized using the torque rheometry technique implemented in the equipment Plastograph (Brabender GmbH & Co. KG). The torque rheometry allows to evaluate the torque value applied to the mixture binder and powder, as a function of the mixing time. The temperature used was 180°C, considering the characteristics of the master binder used. The blade rotations were 30 rpm and the mixing time was over 30 minutes,

when the stability state is normally achieved. The total volume of the mixing chamber is 50 cm^3, however, due to the volume of the blades, the working volume is 38.5 cm^3.

Since the amount of powder in the feedstock plays a fundamental role in the shaping, experimental tests were carried out to evaluate the critical powder volume concentration (CPVC), in order to use the maximum admissible powder volume in the feedstock [37]. As referred in the state of the art, for PIM feedstocks using WC-10Co, the window value is defined as 40 to 70 vol.%, with an average value of 50 vol.% [45]. Since the FDC process uses smaller shear rates than the injection of PIM materials, it was necessary to perform an optimization of CPVC by doing a set of tests using different concentration values.

Several CPVC tests were performed to evaluate the optimal concentration. A range of powder volume was selected (10% interval) and small portions (1% volume) were added until the total volume of the mixing chamber was filled. The first CPVC test was performed using a concentration range between 40 and 50% of the total volume of the mixing chamber but using this range it was not possible to define the CPVC, as the torque value stabilized after each addition of powder and presenting low values, then suggesting that more powder content could be added. On a second CPVC test, the powder range was adjusted with volume concentrations between 43 and 53%. With this powder volume range, the torque variation was unstable, and the torque value increased significantly for volume concentrations higher than 50%, which would negatively affect the flowability of the filament while extruding the green part. After the determination of the maximum powder volume, a control optimization, with values between 45 and 50 vol.%, was performed to analyze the feedstock mixing behavior using the maximum powder concentrations.

As described on section 3.1.1, after the analysis of the TGA of the powder, it was found that the powder had 3 wt.% of paraffinic wax, which represented a lower powder volume than expected. Although it was desired to increase the powder content in the feedstock as much as possible, the tests performed showed that the torque values that allowed the development

of an extrudable filament were already achieved. More results regarding the impact of the wax presence in the feedstock will be given in chapter 4.

3.2.2. Scanning electron microscopy (SEM)

Scanning electron microscopy (SEM) produces images of a sample by scanning the surface with a focused beam of electrons. The electrons interact with atoms in the sample, producing various signals that contain information about the surface topography and composition of the sample [53].

SEM was used to carry out the analysis of the powder distribution along the extruded filament in the 3D equipment, as well as to analyze the topology and defects in the green parts. SEM was performed using a FEI Quanta 400FEG ESEM / EDAX Genesis X4M.

3.2.3. Infinite Focus Microscopy (IFM)

Infinite Focus Microscopy (IFM) presents a non-contact optical 3D measurement technique, with high repeatability and vertical resolution, which provides 3D surface topologic information. This technique allows up to 10 nm on vertical resolution and is based on the focus-variation principle [54].

Different resolutions are guaranteed by different precision lens that can be applied in the equipment. In the present study, measurements were performed using the green prototype and the final part, in order to study the total shrinkage of the part after processing. The measurements were evaluated by IFM technique from Alicona Imaging GmbH.

3.2.4. Ultra-microhardness

After the sintering stage, a hardness measurement technique was performed to evaluate the hardness of the final part. The equipment used was the Fischerscope H100 Ultra-Microhardness Tester. This equipment measures ultra-low hardness under test load, with a load range of 0.4 mN to 1,000 mN and test uncertainties below 1 percent [55]. With the Fischerscope H100, it is possible to control the load and the indentor penetration, such that the effects of the material substrate on measurement results can be virtually eliminated.

Measuring the hardness also allows to calculate the Young's module through the surface deformation obtained. Two different sets of tests were performed, using two different maximum loads, 250 and 500 mN, respectively.

4. Results & Discussion

The present chapter shows the methodology adopted for the experimental development of the study, as well as the results obtained and their discussion. All the different stages of filament development and green part post-processing are approached, as well as the respective characterizations.

4.1. From Powder to Feedstock

As previously described, the evaluation of CPVC is fundamental to obtain a filament with optimized powder content, thus, several optimizations of the powder content were carried out as a function of the obtained torque. The powder was added to the mixing chamber when the mixing torque presented a stable behavior, generally in 10-minute periods.

Figure 18 shows the values of torque obtained in the optimization of the feedstock.

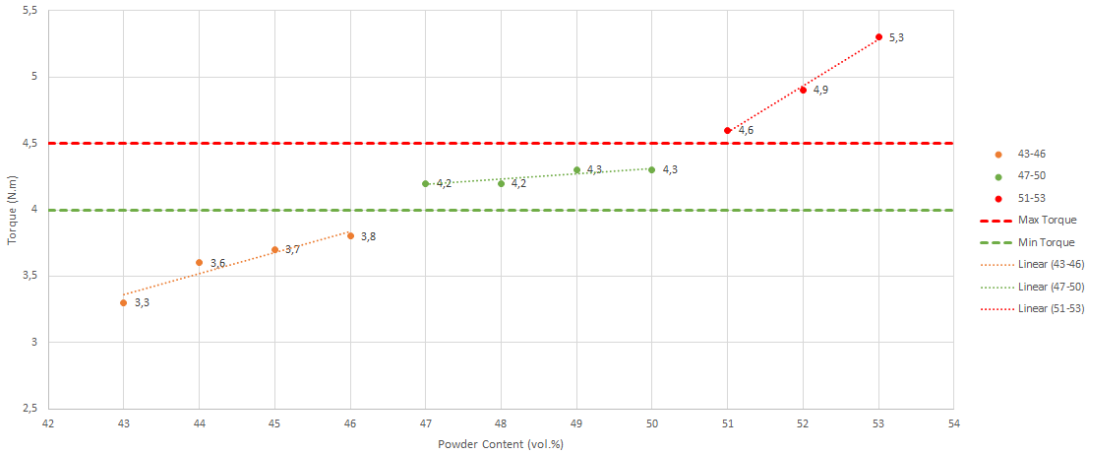

Figure 18 - CPVC optimization for WC-10Co

As it is possible to observe in Figure 18, three different slopes were obtained, as a function of the powder concentration. The optimized torque was defined between 4 and 4.5 N.m [37], corresponding to concentrations between 47 and 50 vol. % of powder. The concentration of

50 vol.% was considered the maximum value, since after this value is visible the torque increase, which could compromise the extrusion process.

After the CPVC evaluation, an optimization was performed, with a shorter working window (45-50 vol.%), in order to evaluate the behavior of the feedstock near the maximum admissible limit, using binder BF2 (Figure 19). As the solids content increased, the torque naturally tended to rise, however, the increase was constant during the addition phase. After the point correspondent to 49 vol.% of solids content, the feedstock began to exhibit a stable behavior, obtaining the final stable values of torque after the addition of 50% of powder. The mixture torque stabilized around 4.3 N.m with 50 vol.% of solids content.

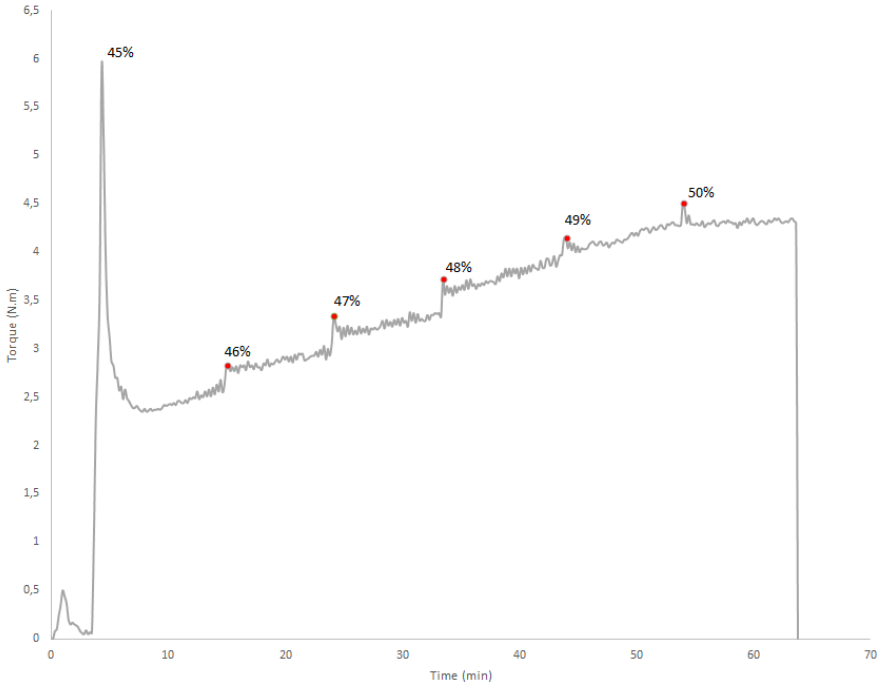

Figure 19 - Final feedstock optimization

After the optimization of the powder content, the feedstock was prepared. Since the desirable torque for the extrusion process should be 4.0 N.m [37], two feedstocks were prepared with 50 vol.% of powder using the binder formulations identified in Table 2 (BF1 and BF2). Using the BF1 binder it was expected a lower torque value, due to the use of stearic acid as

surfactant in this formulation, which should reduce the interparticle forces having a lubrication effect on the powder [37]. However, as can be seen in Figure 20, the binder BF2, although achieving higher torque values in the initial period (7.30-17.30 minutes), tends to stabilized earlier, whereas binder BF1, which contains stearic acid, has lower torques in the same period, but presents a more unstable behavior as time increases. For the same mixing time, approximately 26 minutes, the feedstocks presented the same torque of 4.3 N.m. This behavior may be due to the degradation of stearic acid over the mixing time.

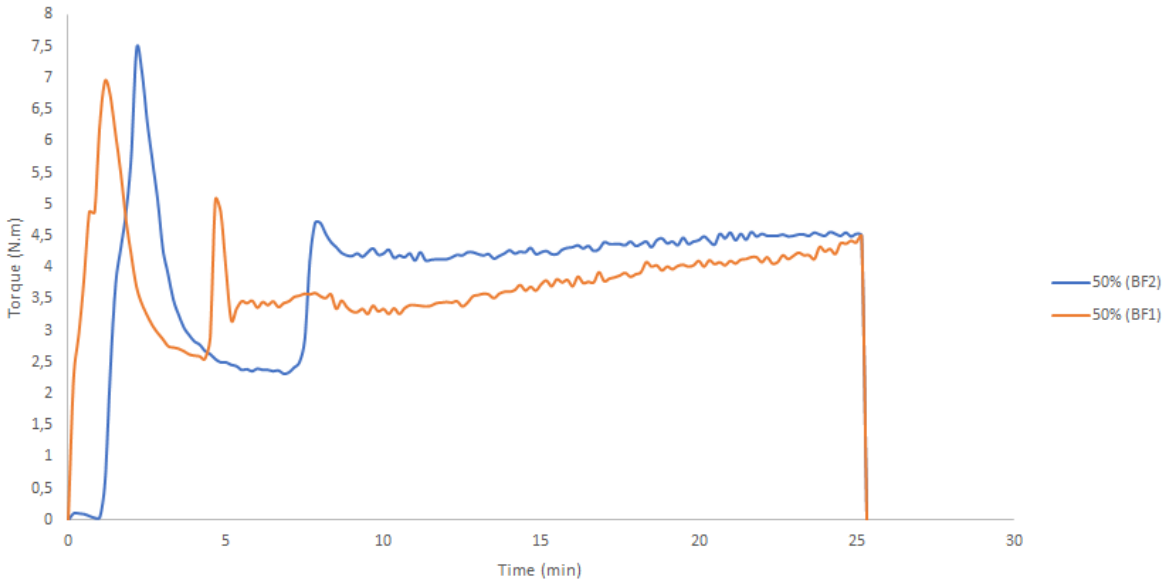

Figure 20 - Feedstock behavior over the mixing time

According the results, three batches of material were produced to prepare the feedstock, using the binder BF2. Figure 21 shows the resulting feedstock after grinding.

Figure 21 - Feedstock after grinding

As described in topic 3.1.1, after the filament extrusion, it was found that the powder had 3%wt. of paraffinic wax, which has a direct impact on the results of CPVC. Although in terms of mass analysis, the difference represents a low amount of mass, due to the difference of the materials density, when considering volume, the difference is more significant. All the work was performed assuming that the powder was non-waxed WC-10Co, meaning that the CPVC real value is not 50 vol.%, as evaluated. Figure 22 shows the CPVC optimization considering the 3 wt.% of paraffinic wax in the feedstock. As it is possible to observe, the CPVC changed from 50 to 48.5 vol.%. Despite the change of the powder content considering the presence of paraffinic wax, as the optimization of the torque was performed in consonance, it is possible to conclude that using this specific powder and binder formulation, it would not be possible to add more powder to the feedstock, maintaining simultaneously torque stability and acceptable torque values.

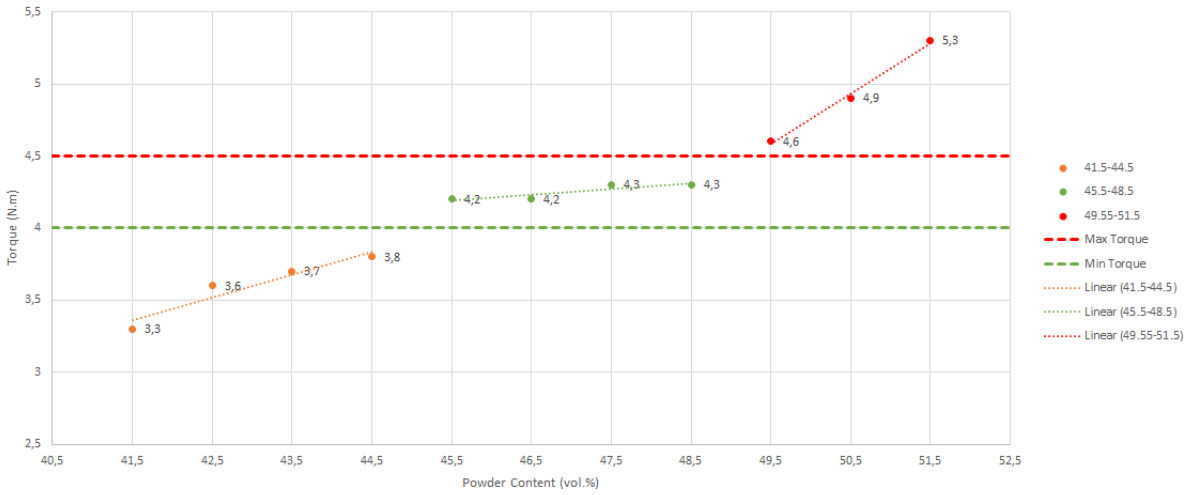

Figure 22 - CPVC optimization for WC-10Co + 3 wt.% paraffinic wax

4.2.From Feedstock to Filament

The present topic adresses the methodology used to obtain a filament and showcases the techniques applied to that filament characterization.

4.2.1. Filament Production

After feedstock preparation the production of filament was the next stage. FDM printers, such as BQ Prusa I3, usually use filament spools with 1.75 mm of diameter as standard measure. In this study, it was not possible to obtain that value because a winding mechanism was needed at the tip of the nozzle to ensure that a constant pulling force and a constant winding speed were applied. The filament diameter was maintained as constant as possible, kepping at the same height during the extrusion the spool where the filament was beeing extruded to.

The filament diameter range was 1.65±0.05 mm. Figure 23 show the spool of filament produced.

Figure 23 - Filament produced

After producing a spool of filament, a small sample was taken for trying its extrusion in the 3D printing machine to test if it was extrudable. A commercial extrusion nozzle of brass based material, coated with nickel composite to decrease wear during extrusion, was used. The nozzle has a standard inner diameter of 0.4 mm. Figure 24 shows the extruded filament using BQ Prusa I3.

Figure 24 - Filament after 3D printer extrusion

4.2.2. Characterization

To ensure that the filament has a good performance during the FDC process, some characterization tests were performed to evaluate the filament homogeneity, density and thermal behavior.

a) Homogeneity

After testing the extrusion on BQ Prusa I3, the filament was analysed to evaluate the homogeneity of the feedstock. A small sample was cutted from the extruded material and was observed using the SEM equipment.

Figure 25 shows a cross section of the printed filament, being visible that the surface has some geometric defects. These defects are due to the fact that the cut of the filament has been done with a scalpel, which introduced small breaks of material at the surface. Although the presence of those defects, the cross section shows that the filament has a constant diameter of 0.42 mm after extrusion by the 3D printer. Figure 26 shows the magnifications of the cross section. In Figure 26(a) is clear that the binder is well distributed in the powder, but in Figure 26(b) and (c) are visible some agglomerates of tungsten carbide and cobalt. This phenomena is due to the fact that cobalt acts like a binder in the WC-Co mixture, what may result in higher densities at specific points in the final produced part.

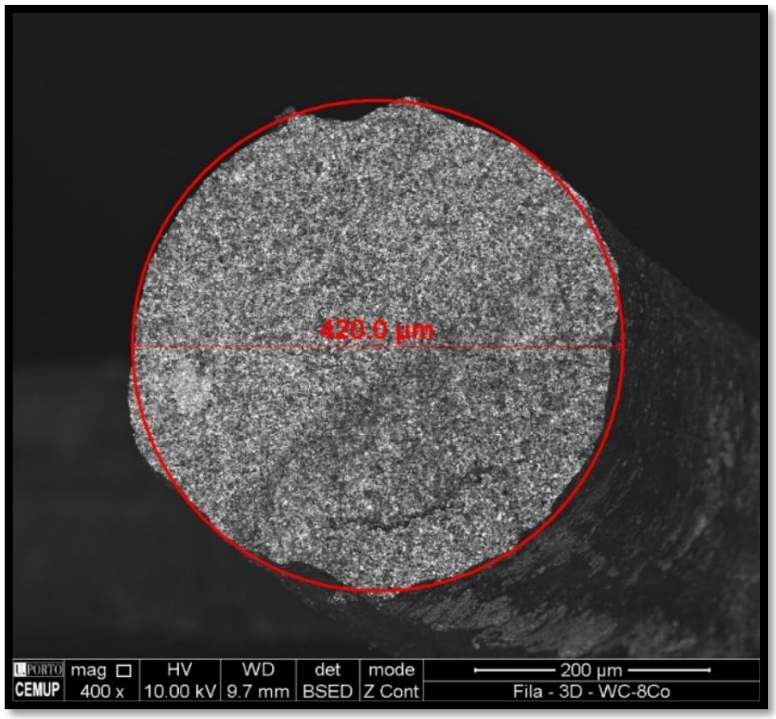

Figure 25 - SEM of the extruded filament (400x)

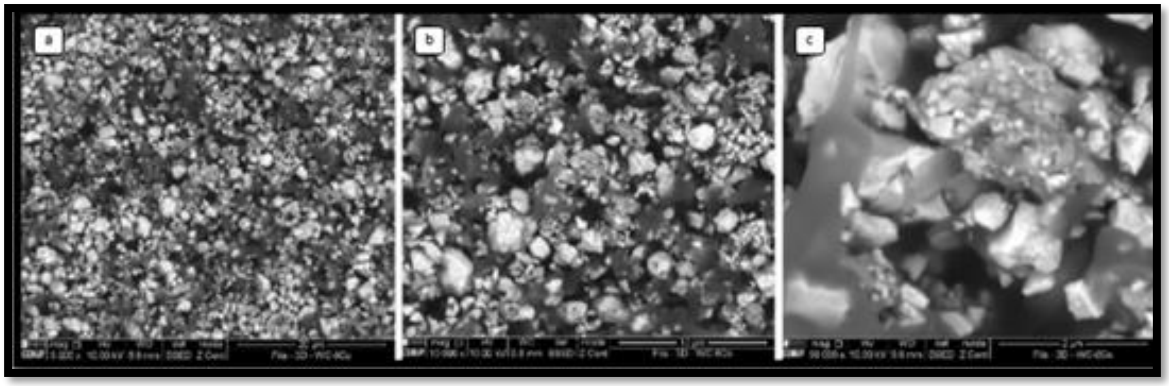

Figure 26 - SEM of the extruded filament: 5000x (a); 10000x (b); 50000x (c)

b) Density

In order to assess the filament density, the mixtures law (equation 1) was applied to determine the theoretical density that was compared with the filament apparent density evaluated by the Archimedes principle.

$$\rho_{\text{feedstock}} = (\text{Vol.}\,\%\ \text{powder} \times \rho_{\text{powder}}) + (\text{Vol.}\,\%\ \text{binder} \times \rho_{\text{binder}}) \quad (1)$$

where,

Vol.% powder = volume fraction of ceramic powder;

Vol.% binder = volume fraction of binder;

ρ_{binder}= density of binder;

ρ_{powder}= density of powder.

Density tests (Table 4) show that the filament apparent density is lower than the density determined using the mixtures law. This difference can be explained with the unaccounted extra wax presence in the powder that the latter TGA performed to the powder revealed.

Table 4 - Theoretical vs Apparent density

	Theoretical	Apparent
Density (kg/m^3)	7880	7100

c) Thermal behavior

Although the individual constituents of the filament were already studied in terms of thermal behavior, it is important to analyze if that behavior is the same when they are mixed in the filament. Performing a TGA on the filament is also important to assess the total powder volume present. Figure 27 shows the results of the filament thermogravimetric analysis.

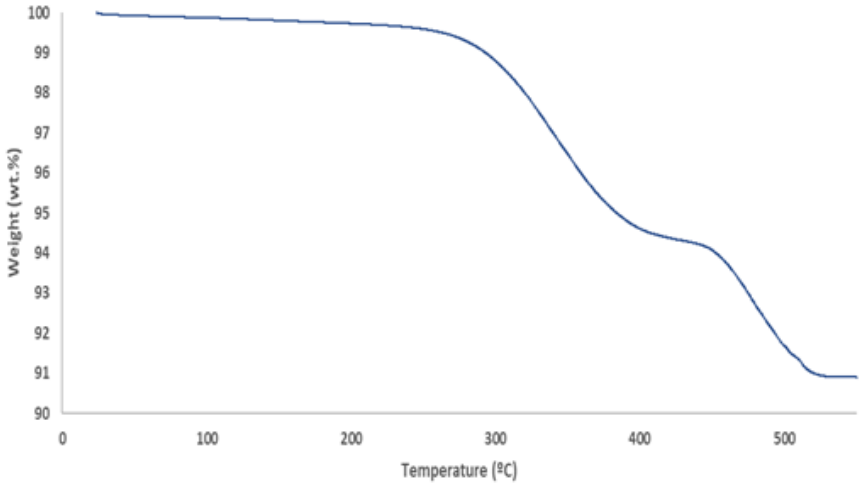

Figure 27 - Filament TGA

Figure 27 shows that 9.5 wt.% was lost in the heating process. The value obtained was 3% higher than expected, suggesting that more polymeric content was present in the filament. Since mass measurements of each constituent were correctly performed, questions about the powder content started to raise. To dissipate uncertainties about the process performed on the development of the feedstock, the TGA of the powder was carried out, reveling that

3wt.% of the powder was paraffinic wax (Figure 16). Apart the extra mass loss, the filament thermal degrading behavior exhibited the same behavior as the previous binder constituents (Figure 17).

4.3.From Filament to Green

The present topic describes the methodology employed to print and characterize the green part produced using the developed filament.

4.3.1. Green part Production

In order to extrude the filament, the BQ Prusa I3 Hephestos printer was used with an extrusion nozzle of diameter 0.4 mm (Figure 28). Eight samples, with different dimensions and geometries, were printed, namely four cylinders and four spur gears. From each set of geometries, two were polished and two were left on their raw state after printing. The main objective was to observe the filament behaviour while printing simple geometries and while printing geometries having tight angles. Regarding polishing,while in a green state, the main objetive was to study the influence of surface finishing on the geometry during sintering.

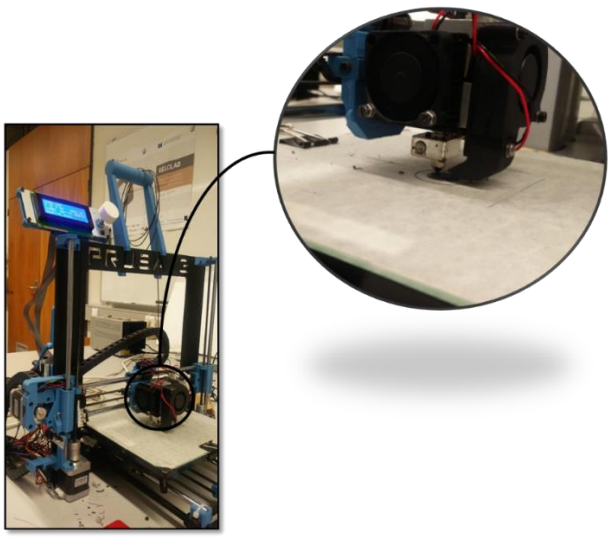

Figure 28 - BQ Prusa I3 Hephestos printing samples

Although the filament had some dimensional deviations due to the lack of a winding mechanism in the filament extrusion equipment, the printer's stepper motors were able to apply the traction force without any problem, resulting in a constant and balanced filament flow. The produced samples are shown in Figure 29. The first six samples (from S1 to S6) were printed using a double perimeter setting on Slic3r software. Usually this option helps promoting a better surface and infill finish, but depending on the geometry, this may not be achieved. Actually, on samples S5 and S6, the double perimeter setting induced defects, because of the tight angles and infill strategies. Therefore, to avoid the obtained defects, it is important to highlight that samples S7 and S8 were printed using an optimized strategy, and that samples S2, S3, S6 and S7 were polished after printing.

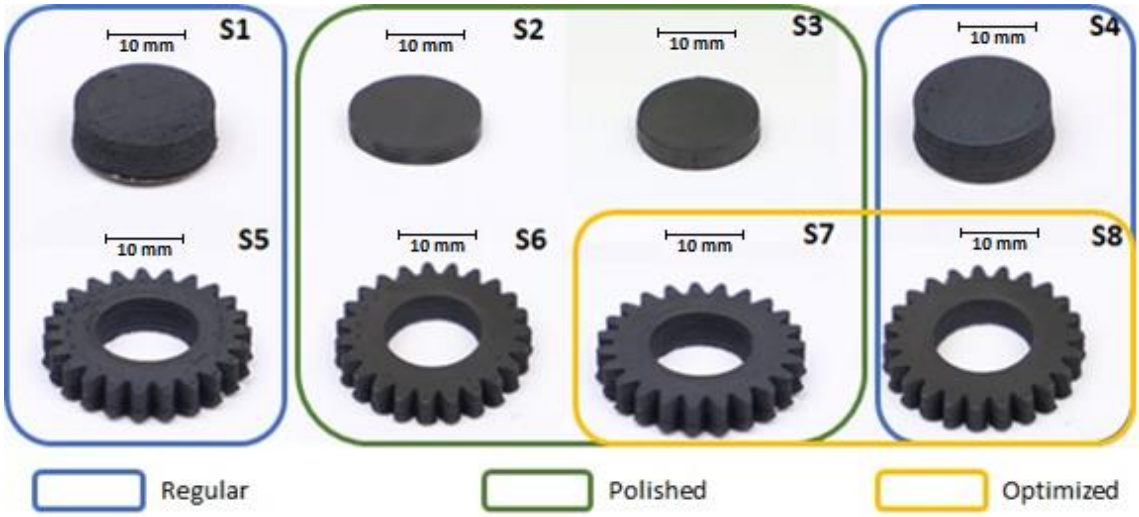

Figure 29 - Produced samples

4.3.2. Characterization

Some defects appeared due to the extruded filament cylinder shape, which is a restriction of this deposition process. After extruding the first perimeter, due to the extruded filament diameter, the minimum feature to be filled has a dimension smaller than 0.4 mm, thus the deposition nozzle can not fill this space, which gives rise to the empty triangle shown in Figure 30. Concerning the union line between the central zone of the spur gear and the region

where the toothing begins (Figure 30), the defect is due to the strategy of filling the part, whose angles of deposition were not optimized for the toothed geometry.

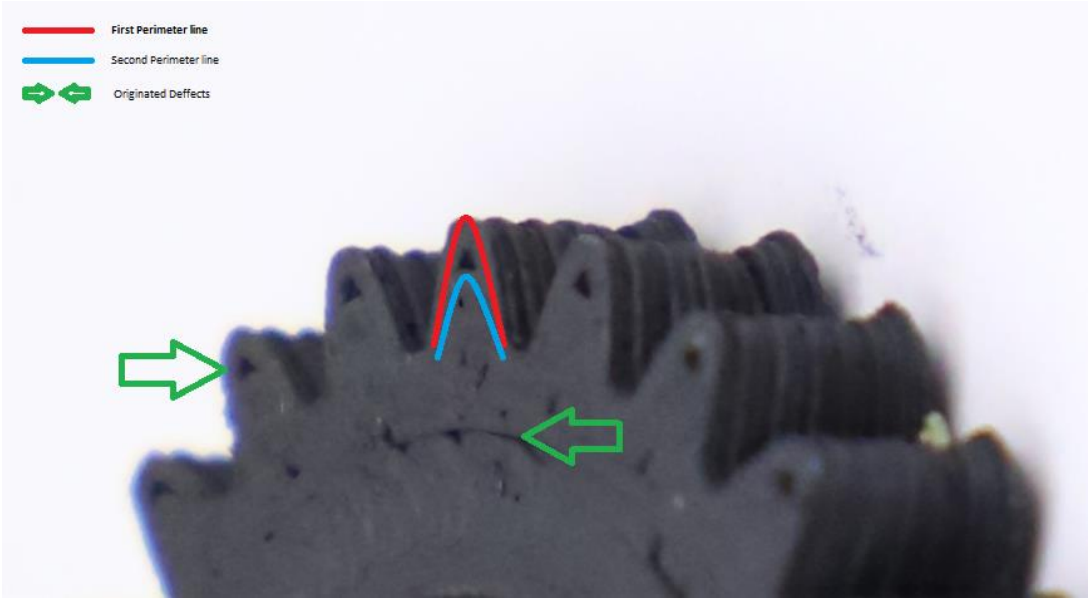

Figure 30 - Double perimeter defects after extrusion

In order to avoid the mentioned defects, which can induce serious structural complications during sintering, and may even cause the collapse of the structure, a simple perimeter and a 45º angled strategy was applied to remove the lack of infill in those points. Figure 31 shows the obtained part applying this strategy (S8 sample).

Figure 31 - S8 Sample obtained with angled and simple perimeter strategy

The green samples after printing were weighed and the diameter and height of each one was also measured using a TESA dial caliper ruler and Kern & Sohn GmbH ABS 220-4 scale. A set 3 measurements were made to each dimension to obtain the average dimension (Table 5).

Table 5 - Samples measurements

Sample	Weight (g)	Dimensions (mm)				
		Out Diameter	Inner Diameter	Height	CAD out diameter	CAD inner diameter
S1	5.30	15.04	-	5.80	15.00	-
S2	2.97	14.99	-	2.80		
S3	3.47	15.09	-	3.20		
S4	5.78	14.98	-	5.89		
S5	8.06	25.40	12.32	5.01	25.00	12.00
S6	7.71	25.10	12.26	4.40		
S7	3.50	24.64	12.21	1.95		
S8	6.04	24.60	12.24	3.60		

The variations obtained in the diameter are related to the processing conditions, namely the overlap between filaments and the boundary conditions (use of only one perimeter). Figure 32 shows schematically the effect of the overlap on the layer's deposition. With an optimized strategy, to avoid creating defects in the FDC process, it is possible to realize that there has been some dragging of the outer filament into the interior of the part, reducing the overall diameter. In parts produced without optimization, using two perimeters, the overall exterior diameter is increased.

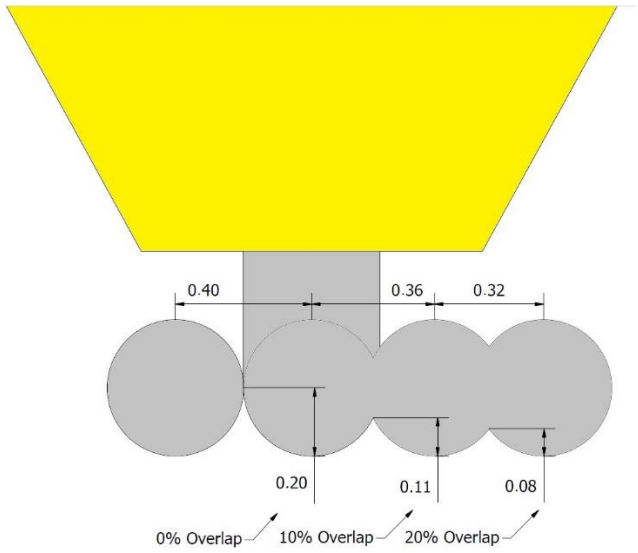

Figure 32 - Overlap effect on layer dimension (dimensions in mm)

4.4.From Green to Final part/System

The present section presents the used sintering conditions and showcases the results obtained thru geometrical and mechanical tests.

4.4.1. Sintering Stage

After printing, the green parts were sintered using a industrial Hot Isostatic Pressing (HIP) sintering oven, in order to obtain the final part. Although thermal studies were performed to the filament and its constituents, to define a controlled removal of each constituent, the company where the sintering tests were performed used its implemented sintering process, doing the proper adjustments to samples based on feedstocks, namely the one used in the present work (WC-10Co+BF2). Samples 1, 6 and 7 were sintered using a sintering cycle with two stages, the first one at 680ºC under hydrogen atmosphere to remove all the waxes and the second one at 1485ºC and 25 bar pressure (profile 1) and samples 2, 5 and 8 were sintered at 1450ºC and 30 bar pressure (profile 2). Different results were obtained while using the different sintering profiles. Table 6 shows the results obtained after sintering, namely in terms of sample weight loss, free Co (using a magnetic scale) and sintering profile.

Table 6 - Sintering results

Sample	$Weight_{initial}$ (g)	$Weight_{final}$ (g)	Weight loss (%)	Free Co (wt.%)	Sintering profile
S1	5.31	4.47 (broke)	10.13	9.39	1
S2	2.97	2.71	8.72	8.88	2
S3	Sintering not performed				
S4	Sintering not performed				
S5	8.06	7.35	8.87	9.06	2
S6	7.71	7.02	8.99	8.08	1
S7	3.49	Broke			1
S8	6.04	5.49	9.05	9.29	2

Both sintering profiles presented a free cobalt percentage above 8wt.%, meaning that approximately 1-2% of cobalt reacted during the sintering process. The parts that were sintered using the sintering profile 1, two out of three, appeared broken after the process was completed. Thus, direct sintering (profile 2) gave rise to parts with more integrity.

Regarding the weight loss, it was expected a value of 6.5wt.%, since the mass fraction of WC-10Co was around 93.5%, but due to the presence of wax on the powder, the loss of weight was close to 9.5%. Figure 33 shows some samples after sintering, where some visible defects are present.

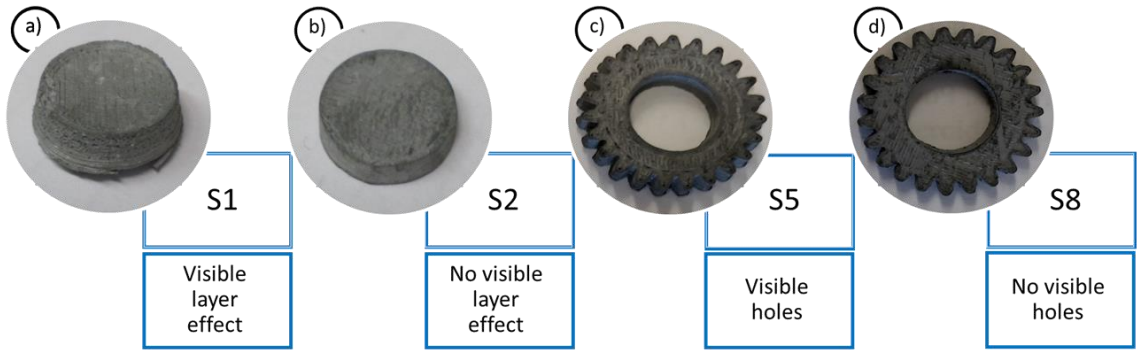

Figure 33 - Samples after sintering: S1 (a); S2 (b); S5 (c); S8 (d); figures a) and b) show the difference between non-polished (S1) and polished (S2) green parts

Concerning the surface finishing after sintering, Figures 34(a) and (b) show the main difference between the non-polished (S1) and polished (S2) samples in the green state. Sample S2 does not display the typical layer effect associated with the FDC process, which is visible on sample S1. Regarding samples S5 and S8 (Figures 34(c) and (d)), defects originated during printing are visible on sample S5, presenting some holes on the tooth area and on the center of the sample. Sample 8 has a similar surface finishing, since no green polishing was applied, but due to the improved printing strategy, there are no visible holes. Samples subjected to green state polishing presented an overall better-quality surface, eliminating the peak effect generated by layer stacking, but proven to be limited to the part geometry, since in complex parts it was not possible to perform an even polishing on all surfaces. The printing strategy was fundamental to obtain parts without process defects, showing that planning the deposition directions, in order to avoid geometrical deposition constrains, have a direct impact in overall part quality.

In order to study the samples hardness, a surface polishing was performed after sintering to obtain a smooth surface (≈1 µm). Figure 34 shows S5 and S8 samples in these conditions, being possible to observe that the defects were minimized through the change on the printing strategy, removing the holes, thus originating better results after sintering.

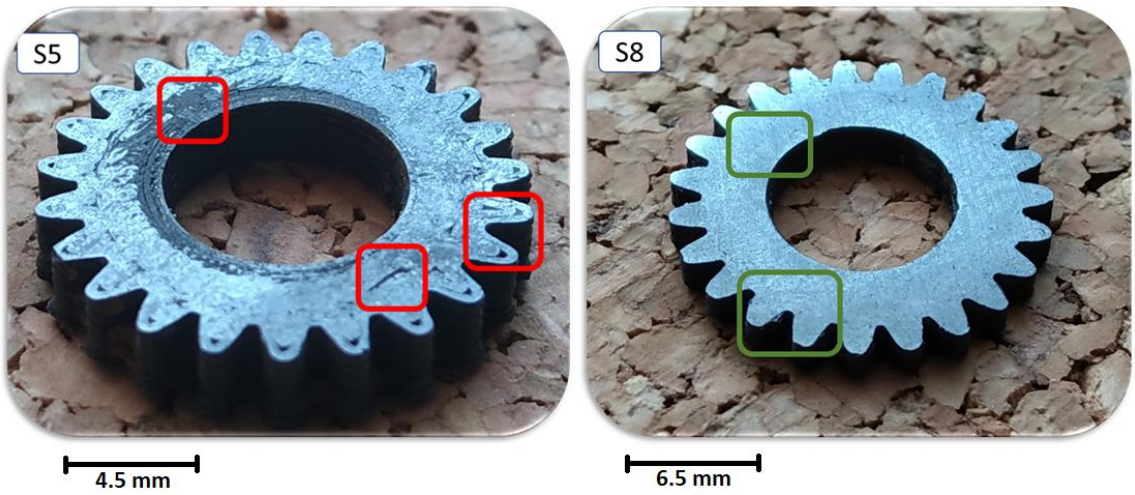

Figure 34 - Difference between non-optimized (S5) and optimized (S8) sintered parts after surface polishing

4.4.2. Dimensional and mechanical characterization

In order to evaluate the results after sintering, shrinkage, hardness and Young's module were evaluated.

a) Shrinkage

To evaluate the final part shrinkage measurements were performed on both the green part, after FDM printing, and on the final part, after sintering, using an IFM technique. Measurements were performed for the different details of the parts, such as internal diameter (D1), external diameter (D2), tooth upper dimension (A), tooth lower dimension (B) and height (H). A set of three measurements were made to obtain the average contraction on these details, which allowed an estimation of the overall part shrinkage. Measurements were performed using samples S5 and S6. Figure 35 illustrates the measurements that were evaluated.

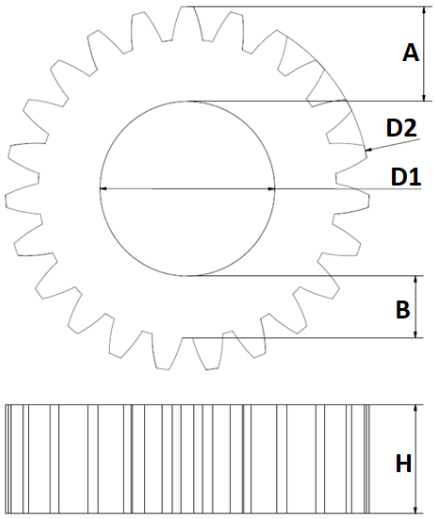

Figure 35 - Measurements scheme

Figure 36 allows to observe the samples evolution during the process with IFM pictures of samples S5 and S6, as well as the overlay picture. Table 7 summarizes all the dimensions obtained on each sample as well as the contractions obtained on those directions.

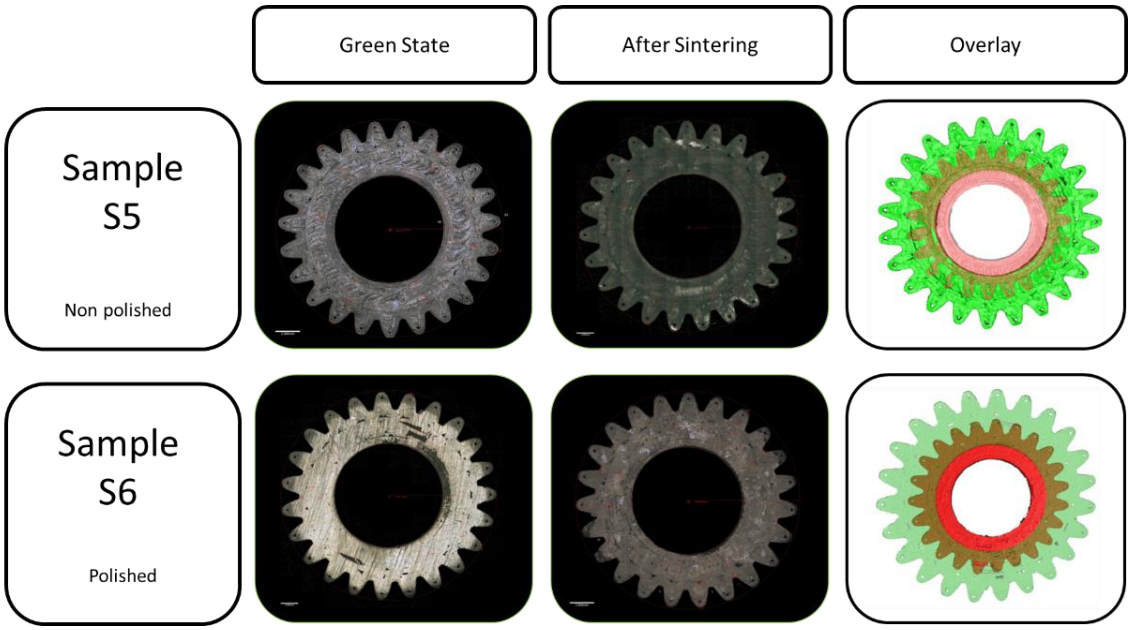

Figure 36 - IFM sample overlay

Table 7 - Measurements and shrinkage after sintering

Measurements	Dimensions (mm)		Shrinkage (%)		Overall Shrinkage (%)	
	S5	S6	S5	S6	S5	S6
D1	8.42	9.05	31.35	26.90		
D2	18.25	18.28	26.53	26.17		
A	4.53	4.48	26.56	26.64	26.56 ± 1.64	26.63 ± 0.39
B	3.03	2.90	25.04	27.33		
H	3.67	3.00	26.70	26.10		

Measurements of both samples allowed to conclude that the shrinkage after sintering was homogeneous in all its directions, except D1 on sample S5, resulting in an overall shrinkage of 26.56% and 26.63% in samples S5 and S6, respectively. Studies regarding linear shrinkage show that for WC-10Co with a CPVC of 50 vol.%, the linear shrinkage observed was 22% [45]. The higher values obtained on the present work may be due to the uncounted wax content of the powder and also due to the use of a powder with different particle size.

Regarding the difference between non-polished (S5) and polished green parts (S6), no significant differences were noticed, since shrinkage percentage was almost the same, having just a smaller variation on S6 sample.

b) Hardness & Young's Modulus

To measure the hardness of the produced parts, 20 measurements were performed on samples S5 and S6 using the Fischerscope H100 equipment. A load of 250 mN was used for the first 10 measurements and 500 mN for the last 10 measurements. The penetration measurements allowed to determine the average hardness of the samples. The behavior of the sample while deforming allowed to evaluate the average Young's module. The measurements were made in different sections of the part surface to ensure that they were representative of the overall part characteristics. Table 8 summarizes the combined average

hardness and Young modulus of the samples and also presents results of the literature for a WC sample. The hardness and Young modulus are within the literature expected values for tungsten carbide [56] and for tungsten carbide with cobalt [57].

Table 8 - Samples average Hardness and Young Modulus

Sample	Hardness (GPa)	Young Modulus (GPa)
WC-10Co*	19.8 ± 2.4	678 ± 72
WC**	12.8 – 21.6	669-696
WC-10Co***	16.4 – 18.2	-
Measured; **Literature** [56];Literature**[57]		

5. Conclusions and future work

The main objective of the present study, to develop a ceramic filament suitable for FDC, was achieved, using the methodology explained on the previous chapters. Filament characterization was also presented, showing the main filament properties.

Materials selection, in particular binder formulations, played a vital role on the development of this study, since it allowed obtaining a filament with rheological properties suitable for FDC printing. The binder formulation was responsible for obtaining a filament with enough strength to maintain shape while printing, but also to have enough flexibility to withstand bending and rolling into a spool. TGA performed to the binder constituents and to the filament showed that all the polymeric material was degraded, leaving only the ceramic material. Powder characterization also had an important role on the filament, since the particle size distribution was responsible to ensure that a good and homogenous powder distribution was presented in the feedstock. TGA performed to the powder was also fundamental to understand why an extra mass of polymeric material was lost during the thermogravimetric tests and sintering.

The CPVC determination technique used in the present study allowed to obtain precise results of the maximum powder content (1% volume uncertainty), which originated filaments with optimized powder content. The obtained CPVC was not the real one, since only after doing TGA test to the filament it was noticed that the powder had some wax content. Despite the real value being 48.5 vol.% instead of 50 vol.%, it was concluded that the optimized mixing torque of the feedstock that was used on the filament development was already achieved, meaning that for the studied powder (WC-10Co + 3wt.%wax) the powder content was the most adequate.

The filament developed was successfully extruded using a FDC process, being able to produce simple geometries, such as cylinders, as well as a more complex part, spur gear. The filament displayed a good flowability while maintaining the structural integrity, making it suitable for FDC processing. FDC process parameters also had an impact on the overall

quality of the part, showing that for complex geometries, with tight angles, is important to adequate the printing strategy to obtain a better infill, decreasing the possibility of obtaining defects after sintering.

Results obtained after sintering, despite not being possible to apply the thermal debinding stages previewed by the TGA tests, revealed that the green part had a homogeneous distribution of powder, since the parts shrinkage was constant along the three axes. Although the shrinkage value was higher than the ones presented in the literature, the powder content was higher, justifying the extra shrinkage obtained. Hardness and Young's module measurements were within the typical values for tungsten carbide across the entire sample.

Based on the present study, the future research works could focus on:

- Perform a comparison study between waxed and non-waxed powders, using tungsten carbide;
- Compare powder concentrations using different extrusion mechanisms (plunge vs. feedstock vs. filament);
- Compare different backbone polymers and binder formulations;
- Perform FDC extrusion with different diameters;
- Study the densification and porosity after sintering;
- Study the influence of sintering on layer interface;
- Microstructural evaluation of sintered parts;
- Rheological properties of filament.

6. Bibliography

[1] Wroe, J. (2015). Introduction to Additive Manufacturing Technology: A Guide for Designers and Engineers. European Powder Metallurgy Association.

[2] Gibson, I., Rosen, D. W., & Stucker, B. (2010). Additive manufacturing technologies: Rapid prototyping to direct digital manufacturing. Additive Manufacturing Technologies: Rapid Prototyping to Direct Digital Manufacturing. Springer US.

[3] W. Koff and P. Gustafson (2012). 3D Printing and the Future of Manufacturing. CSC Lead. Edge Forum, no. June, pp. 1–11.

[4] Gu, D. (2015). Laser additive manufacturing of high-performance materials. Laser Additive Manufacturing of High-Performance Materials. Springer Berlin Heidelberg.

[5] Wohlers, T. (2005). Early Research & Development. Wohlers Report 2005- Rapid Prototyping, Tooling & Manufacturing State of the Industry (pp. 1–7).

[6] Bártolo, P. (2011). Stereolithography: Materials, Processes and Applications. Springer Germany

[7] Wohlers, T.(2017). History of Additive Manufacturing. (pp. 1–24).

[8] Wohlers, T. (2016). Wohlers Report 2016 - 3D Printing and Additive Manufacturing State of the Industry (pp. 140–148).

[9] Chua, C.K., Leong, K. F., Lim, C.S. (2010) Rapid Prototyping: Principles and Applications. World Scientific.

[10] German, K.F., Hens, R.M. (1991) Key Issues in Powder Injection Molding, Ceramic Bulletin, vol. 70, no. 8, (pp. 1294–1302).

[11] German, K.F. (1993). Powder Injection Molding, Metal powder industries federation.

[12] Gnanamuthu, D.S. (1976). Cladding. US Patent No. 3952180, (pp. 121-219).

[13] Ngo, T. D., Kashani, A., Imbalzano, G., Nguyen, K. T. Q., & Hui, D. (2018, June 15). Additive manufacturing (3D printing): A review of materials, methods, applications and challenges. Composites Part B: Engineering. Elsevier Ltd.

[14] Hopkinson, N & Hague, Richard & Dickens, Philip. (2006). Rapid Manufacturing: An Industrial Revolution for the Digital Age. Wiley.

[15] Eyers, D. R., & Potter, A. T. (2017). Industrial Additive Manufacturing: A manufacturing systems perspective. Computers in Industry, (pp.92–93, 208–218).

[16] Sossou, G., Demoly, F., Montavon, G., & Gomes, S. (2018). An additive manufacturing oriented design approach to mechanical assemblies. Journal of Computational Design and Engineering, 5(1), (pp. 3–18).

[17] Crump, S. S. (1992). Apparatus and method for creating three-dimensional objects. US Patent No. 005121329.

[18] Kun, K. (2016). Reconstruction and development of a 3D printer using FDM technology. In Procedia Engineering (Vol. 149, pp. 203–211). Elsevier Ltd.

[19] Kim, Y., Lee, J., & Oh, J. H. (2018). Fabrication of fine metal patterns using an additive material extrusion process with a molten metal. Microelectronic Engineering, 191, (pp.10–15).

[20] Onagoruwa, S., Bose, S., & Bandyopadhyay, A. (2001). Fused Deposition of Ceramics (FDC) and Composites. In Proceedings of the Solid Freeform Fabrication Symposium (pp. 224–231).

[21] Nikzad, M., Masood, S. H., & Sbarski, I. (2011). Thermo-mechanical properties of a highly filled polymeric composites for Fused Deposition Modeling. Materials and Design, 32(6), (pp. 3448–3456).

[22] Sajan, N., John, T. D., Sivadasan, M., & Singh, N. K. (2018). An investigation on circularity error of components processed on Fused Deposition Modeling (FDM). In Materials Today: Proceedings (Vol. 5, pp. 1327–1334). Elsevier Ltd.

[23] Pham, D. T., & Gault, R. S. (1998). A comparison of rapid prototyping technologies. International Journal of Machine Tools and Manufacture, 38(10–11), (pp.1257–1287).

[24] Prakash, K. S., Nancharaih, T., & Rao, V. V. S. (2018). Additive Manufacturing Techniques in Manufacturing -An Overview. In Materials Today: Proceedings (Vol. 5, pp. 3873–3882). Elsevier Ltd.

[25] Additively, "Fused Deposition Modeling," 2018. [Online]. Available:https://www.additively.com/en/learn-about/fused-deposition-modeling. [Accessed: 20-Mar-2018].

[26] Statista, "Most used 3D printing technologies in 2017 and 2018," Technology and Telecomunications,2019.[Online].
Available:https://www.statista.com/statistics/756690/worldwide-most-used-3d-printing-technologies/. [Accessed: 20-Mar-2018].

[27] Agarwala, M. K., Bandyopadhyay, A., Van Weeren, R., Langrana, N. A., Safari, A., Danforth, S. C., … Pollinger, J. (1996). Fused Deposition of Ceramics (FDC) for Structural Silicon Nitride Components. In Proceedings of Solid Freeform Fabrication Symposium (pp. 335–344).

[28] Gibson, I., Rosen, D. W., & Stucker, B. (2010). Additive manufacturing technologies: Rapid prototyping to direct digital manufacturing. Additive Manufacturing Technologies: Rapid Prototyping to Direct Digital Manufacturing(pp. 1–459). Springer US.

[29] Montagu, J., Configurations, M., Deflection, B., and Technologies, S. (1998). Solid Freeform Fabrication Methods, US Patent No 5738817.

[30] V. P. Lindsay. (2016). Feasibility of Fused Deposition of Ceramics with Zirconia and Acr, Faculty of California Polytechnic State University.

[31] Kruth, J. P., Leu, M. C., & Nakagawa, T. (1998). Progress in additive manufacturing and rapid prototyping. CIRP Annals - Manufacturing Technology, 47(2), (pp.525–540).

[32] Safari, A. (2001). Processing of advanced electroceramic components by fused deposition technique. In Ferroelectrics,Vol. 263, (pp. 45–54).

[33] Agarwala, M. K., Weeren, R. V., Bandyopadhyay, A., Safari, A., Danforth, S. C., & Priedeman, W. R. (1996). Filament Feed Materials for Fused Deposition Processing of Ceramics and Metals. Proceedings Ofthe Solid Freeform Fabrication Symposium,712,(pp. 451–458).

[34] Rangarajan, S., Qi, G., Venkataraman, N., Safari, A., & Danforth, S. C. (2010). Powder Processing, Rheology, and Mechanical Properties of Feedstock for Fused Deposition of Si3N4 Ceramics. Journal of the American Ceramic Society, 83(7), (pp.1663–1669).

[35] Bellini, A., Shor, L., & Guceri, S. I. (2005). New developments in fused deposition modeling of ceramics. Rapid Prototyping Journal, 11(4), (pp.214–220).

[36] Gonzalez-Gutierrez, J., Cano, S., Schuschnigg, S., Kukla, C., Sapkota, J., & Holzer, C. (2018, May 18). Additive manufacturing of metallic and ceramic components by the material extrusion of highly-filled polymers: A review and future perspectives. Materials. MDPI AG.

[37] F. Barreiros, “Optimização da moldação por injecção de pós de resíduos industriais inorgânicos,” Universidade de Coimbra - Faculdade de Ciências e Tecnologia, 2002.

[38] Shukla, V. N., & Hill, D. C. (1989). Binder Evolution from Powder Compacts: Thermal Profile for Injection-Molded Articles. Journal of the American Ceramic Society, 72(10), (pp.1797–1803).

[39] Liu, D. M., & Tseng, W. J. (1998). Influence of debinding rate, solid loading and binder formulation on the green microstructure and sintering behaviour of ceramic injection mouldings. Ceramics International, 24(6), (pp.471–481).

[40] Zauner, Rudolf & F. Heaney, Donald & C. Piemme, Jobe & Binet, Chantal & German, Randall. (2002). The Effect of Powder Type and Powder Size on Dimensional Variability in PIM. Powder Metallurgy, Taylor & Francis, vol. 47, (pp. 144-149)

[41] Gonzlez-Gutirrez, J., Beulke, G., & Emri, I. (2012). Powder Injection Molding of Metal and Ceramic Parts. In Some Critical Issues for Injection Molding. InTech.

[42] Atre, S. V., Weaver, T. J., & German, R. M. (2010). Injection Molding of Metals and Ceramics. In SAE Technical Paper Series (Vol. 1). SAE International.

[43] Zhu, B., Qu, X., & Tao, Y. (2002). Powder injection molding of WC-8%Co tungsten cemented carbide. International Journal of Refractory Metals and Hard Materials, 20(5–6), (pp.389–394).

[44] K. S. Nikolaus NESTLE, Marie-Claire Hermant. (2016). Mixture for use in a fused filament fabrication process. WO Patent Nº 2016012486.

[45] Fayyaz, A., Muhamad, N., Sulong, A. B., Yunn, H. S., Amin, S. Y. M., & Rajabi, J. (2015). Micro-powder injection molding of cemented tungsten carbide: Feedstock preparation and properties. Ceramics International, 41(3), (pp.3605–3612).

[46] Kukla, C., Duretek, I., Schuschnigg, S., Gonzalez-Gutierrez, J., & Clemens, H. (2016). Properties for PIM Feedstocks Used in Fused Filament Fabrication. World PM2016, 12(November).

[47] G. S. Upadhyaya (2002) Sintered metallic and ceramic materials — preparation, properties and applications. Materials & Design, 22(4), (pp.329–330).

[48] Rahaman, M. N. (1996). Ceramic processing and sintering. International Materials Reviews,Vol. 41, (pp. 36–37).

[49] Oliveira, R. V. B., Soldi, V., Fredel, M. C., & Pires, A. T. N. (2005). Ceramic injection moulding: Influence of specimen dimensions and temperature on solvent debinding kinetics. Journal of Materials Processing Technology, 160(2), (pp.213–220).

[50] “Mastersizer 3000 laser particle size analyzer,” 2019. [Online]. Available: https://www.malvernpanalytical.com/en/products/product-range/mastersizer-range/mastersizer-3000. [Accessed: 18-Feb-2019].

[51] Carleton College, “X-ray Powder Diffraction (XRD),” 2019. [Online]. Available: https://serc.carleton.edu/research_education/geochemsheets/techniques/XRD.html. [Accessed: 18-Feb-2019].

[52] Rajisha, K. R., Deepa, B., Pothan, L. A., & Thomas, S. (2011). Thermomechanical and spectroscopic characterization of natural fibre composites. In Interface Engineering of Natural Fibre Composites for Maximum Performance (pp. 241–274). Elsevier Ltd.

[53] Carleton College, “Scanning Electron Microscopy (SEM),” 2019. [Online]. Available:https://serc.carleton.edu/research_education/geochemsheets/techniques/SEM.html. [Accessed: 18-Feb-2019].

[54] Alicona, “Infinite Focus | Dimensional metrology & surface roughnes | Alicona - Optical 3D Measurement Technology,” 2019. [Online]. Available: https://www.alicona.com/en/products/infinitefocus/. [Accessed: 18-Feb-2019].

[55] IndustrySearch, “Fischerscope® H100 - Industry Search Australia,” 2019. [Online]. Available: https://www.industrysearch.com.au/fischerscope-h100/p/52237. [Accessed: 18-Feb-2019].

[56] Bauccio, M. (1994). ASM engineered materials reference book. ASM International (p. 580).

[57] Lino, F. J., Guimarães, J., Teixeira, L., Baptista, A. M., & Fernandes, T. (2009). Comparison of Different Cemented Tungsten Carbides Applied to Particleboard Machining End Mills. Proceedings of the Euro International Powder Metallurgy Congress and Exhibition, Euro PM 2009.